Oncogene (2010) 29, 2070–2082

www.nature.com/onc

ORIGINAL ARTICLE

Involvement of JNK in the regulation of autophagic cell death

S Shimizu[1,2], A Konishi[3], Y Nishida[1,2], T Mizuta[2], H Nishina[4], A Yamamoto[5] and Y Tsujimoto[1]

[1]Department of Medical Genetics, Osaka University Medical School, Yamada-oka, Suita, Osaka, Japan; [2]Department of Pathological Cell Biology, Medical Research Institute, Tokyo Medical and Dental University, Yushima, Bunkyo-ku, Tokyo, Japan; [3]Medical Top Track Program, Medical Research Institute, Tokyo Medical and Dental University, Yushima, Bunkyo-ku, Tokyo, Japan; [4]Department of Developmental and Regenerative Biology, Medical Research Institute, Tokyo Medical and Dental University, Yushima, Bunkyo-ku, Tokyo, Japan and [5]Department of Bio-Science, Nagahama Institute of Bio-Science and Technology, Nagahama, Japan

Programmed cell death is a crucial process in the normal development and physiology of metazoans, and it can be divided into several categories that include type I death (apoptosis) and type II death (autophagic cell death). The Bcl-2 family proteins are well-characterized regulators of apoptosis, among which multidomain pro-apoptotic members (such as Bax and Bak) function as a mitochondrial gateway at which various apoptotic signals converge. Although embryonic fibroblasts from Bax/Bak double-knockout (DKO) mice are resistant to apoptosis, we have previously reported that these cells still die by autophagy in response to various death stimuli. In this study, we found that jun N-terminal kinase (JNK) was activated in etoposide- and staurosporine-treated, but not serum-starved, Bax/Bak DKO cells, and that autophagic cell death was suppressed by the addition of a JNK inhibitor and by a dominant-negative mutant of JNK. Studies with sek1$^{-/-}$mkk7$^{-/-}$ cells revealed that disruption of JNK prevented the induction of autophagic cell death. Co-activation of JNK and autophagy induced autophagic cell death. Activation of JNK occurred downstream of the induction of autophagy, and was dependent on the autophagic process. These results indicate that JNK activation is crucial for the autophagic death of Bax/Bak DKO cells.

Oncogene (2010) **29**, 2070–2082; doi:10.1038/onc.2009.487; published online 18 January 2010

Keywords: JNK; autophagic cell death; Atg5

Introduction

Programmed cell death is a genetically regulated mechanism of cell death, which is essential for various biological events, such as morphogenesis and the elimination of potentially harmful cells. Apoptosis is a representative form of programmed cell death, which is regulated by the Bcl-2 family proteins and driven by a family of cysteine proteases called caspases, which have already been intensively investigated. In addition, accumulating evidence suggests that other mechanisms may also contribute to programmed cell death. One of these non-apoptotic death mechanisms may be the so-called 'autophagic cell death' or type II programmed cell death, which is morphologically defined as deaths of cells associated with autophagic changes (Clarke, 1990; Baehrecke, 2002).

Autophagy is an evolutionarily conserved process, which operates constitutively to allow bulk degradation of cellular constituents and organelles in healthy cells, and it is induced above basal levels in response to various stimuli that include starvation, genotoxic stress and deprivation of cytokines (Ohsumi, 2001; Mizushima *et al.*, 2002; Klinonsky, 2005). During the process of autophagy, cellular cytoplasm and organelles are engulfed by double-membrane vesicles called autophagosomes that fuse with lysosomes to become autolysosomes, in which the cargo of the autophagosomes are degraded by lysosomal enzymes. Studies performed in yeasts have revealed more than 30 molecules that are involved in autophagy, including Atg5 and Atg6 (also called Beclin 1), and homologues for these molecules have been found in mammals, providing us with clues to study the physiological process of autophagy (Ohsumi, 2001; Mizushima *et al.*, 2002; Klinonsky, 2005).

Autophagy is primarily a pro-survival mechanism, but there is evidence to suggest that it also functions as a pro-death mechanism under certain conditions (Levine and Yuan, 2005). We previously discovered that embryonic fibroblasts from Bax/Bak double-knockout (DKO) mice are resistant to apoptosis, but still die in a non-apoptotic manner with autophagic features after death stimulation (Shimizu *et al.*, 2004). We have also shown that such non-apoptotic death of Bax/Bak DKO cells is suppressed by inhibitors of autophagy, including a type III phosphoinositide-3 kinase inhibitor, 3-methyl adenine (3-MA), and is dependent on autophagic proteins, such as Atg5 and Beclin 1, indicating that this form of cell death occurs through autophagic machinery (Shimizu *et al.*, 2004). Similarly, Lenardo and colleagues

Correspondence: Professor S Shimizu or Professor Y Tsujimoto, Department of Pathological Cell Biology, Medical Research Institute, Tokyo Medical and Dental University, Yushima, 1-5-45, Bunkyo-ku, Tokyo 103-5802, Japan, or Department of Medical Genetics, Osaka University Medical School, 2-2 Yamadaoka, Suita, Osaka 565-0871, Japan.
E-mails: shimizu.pcb@mri.tmd.ac.jp or tsujimot@gene.med.osaka-u.ac.jp
Received 22 July 2009; revised 17 November 2009; accepted 7 December 2009; published online 18 January 2010

have demonstrated the induction of autophagic cell death when L929 cells were treated with benzyloxycarbonyl-Val-Ala-Asp (OMe) fluoromethylketone (zVAD-fmk), a broad-spectrum caspase inhibitor (Yu *et al.*, 2004). Similar to etoposide-treated Bax/Bak DKO mouse embryonic fibroblasts (MEFs), zVAD-fmk-treated L929 cells die of autophagy, and this form of cell death is blocked by silencing of Atg7 and Beclin 1 (Yu *et al.*, 2004). In both cases, molecules involved in autophagy apparently promote cell death rather than cell survival. When cells are starved, death eventually occurs because of autophagy, but it does not depend on autophagic proteins. Therefore, there are two kinds of autophagy-related cell death, with one being dependent on autophagy and the other being death that is not driven by autophagy. To understand the physiological and pathological roles of autophagic cell death, particularly the autophagy-dependent form of death, it is necessary to elucidate how autophagic molecules are involved in cellular destruction and to find the other molecules that also have a role in this form of cell death. Accordingly, we searched for molecules that were involved in the autophagic death of Bax/Bak DKO MEFs. As a result, we demonstrated that activation of jun N-terminal kinase (JNK) was required for the autophagic death of these cells and that such activation occurred downstream of the autophagic process itself.

Results

Phosphorylation of JNK during etoposide-induced and staurosporine-induced autophagic death of Bax/Bak DKO MEFs

Recently, we showed that various apoptotic stimuli, including etoposide and staurosporine, were able to induce the autophagic death of Bax/Bak DKO MEFs (Shimizu *et al.*, 2004), in which mitochondria-mediated apoptosis signaling is blocked. However, detailed mechanisms underlying this form of cell death were unclear. As JNK was reported to have a crucial role in inducing the autophagic death of zVAD-fmk-treated L929 cells (Yu *et al.*, 2004), we assumed that JNK might act as a pivotal signaling molecule for etoposide (or staurosporine)-induced autophagic death of Bax/Bak DKO MEFs. As shown in Figure 1, the activation of JNK was detected in etoposide-treated Bax/Bak DKO MEFs by the *in vitro* kinase assay (Figure 1a) and by western blot analysis of phospho-JNK (Figure 1b). Addition of SP600125, a JNK inhibitor, prevented the phosphorylation of JNK (Figure 1b). Similar results were obtained with staurosporine (Figure1a; data not shown). Although phosphorylated/active JNK showed molecular sizes of both 46 and 54 kD on western blotting, the 46-kD phosphorylated JNK was dominant in etoposide-treated and staurosporine-treated Bax/Bak DKO MEFs (Figure1b; data not shown). Etoposide caused immediate and sustained activation of JNK with a peak after 3–4 h. Sustained activation of JNK is reported to be linked with cell death (Ventura *et al.*, 2006). Unlike JNK, we did not detect activation of other stress-related mitogen-activated protein kinases, such as p38, extracellular ligand-regulated kinase (ERK)1/2 and ERK5 (Figures 1c–e). These results indicated that JNK was activated in Bax/Bak DKO MEFs by etoposide or staurosporine treatment.

Involvement of JNK in etoposide-induced and staurosporine-induced autophagic death of Bax/Bak DKO MEFs

As JNK was activated in etoposide-treated and staurosporine-treated Bax/Bak DKO MEFs, we next investigated whether its activation was required for etoposide-induced and staurosporine-induced death of Bax/Bak DKO MEFs. As shown in Figure 2a, etoposide-treated Bax/Bak DKO MEFs became rounded and detached from the culture dish, consistent with our previous findings (Shimizu *et al.*, 2004). These cells showed loss of viability when assessed by staining with propidium iodide (PI; a membrane-impermeable stain for nucleic acid staining; Figures 2b and c), as well as by the colony formation assay (Figure 2d) and the cell growth assay using Cell Titer Blue (CTB) to measure the metabolic activity of viable cells (Figure 2e). When Bax/Bak DKO MEFs were treated with etoposide in the presence of 3-MA (an inhibitor of autophagy through type III phosphoinositide-3 kinase), both morphological changes and cell viability were markedly improved (Figures 2a–e), which was also consistent with our previous observations (Shimizu *et al.*, 2004). When SP600125 was added instead of 3-MA, cell rounding and detachment were inhibited, but to lesser extent than with 3-MA (Figure 2a). Similarly, cell viability (assessed by PI staining, colony formation and cell growth) was improved by the addition of JNK inhibitor in a dose-dependent manner, but to a lesser extent than that caused by the addition of 3-MA (Figures 2b–e). Similar results were obtained with staurosporine (Figure 2f). In contrast, a p38 inhibitor (SB203580) and an ERK1/2 inhibitor (U0126) did not have any influence on the extent of autophagic cell death (Figure 2c), a finding consistent with the lack of p38 activation and ERK1/2 activation by etoposide (Figures 1c and d).

For further confirmation of the role of JNK, a dominant-negative form of JNK was expressed in Bax/Bak DKO MEFs to specifically inhibit JNK activation (Figure 2g). As shown in Figures 2h and i, etoposide-induced autophagic death of Bax/Bak DKO MEFs was significantly suppressed by transfection with the dominant-negative JNK plasmid, but not the empty vector, as assessed by PI staining and the CTB assay, confirming the involvement of JNK in autophagic cell death.

To investigate the involvement of JNK in autophagic cell death from another perspective, we used a genetic approach. Activation of JNK requires phosphorylation of both tyrosine (^{185}Tyr) and threonine (^{183}Thr), and two kinases (SEK1 (also known as MKK4) and MKK7 (SEK2)) are essential for the phosphorylation of these amino-acid residues. Therefore, JNK activation is completely abolished in $sek1^{-/-}$ $mkk7^{-/-}$ cells (Nishitai *et al.*, 2004). As we previously demonstrated that, similar to Bax/Bak DKO MEFs, MEFs overexpressing

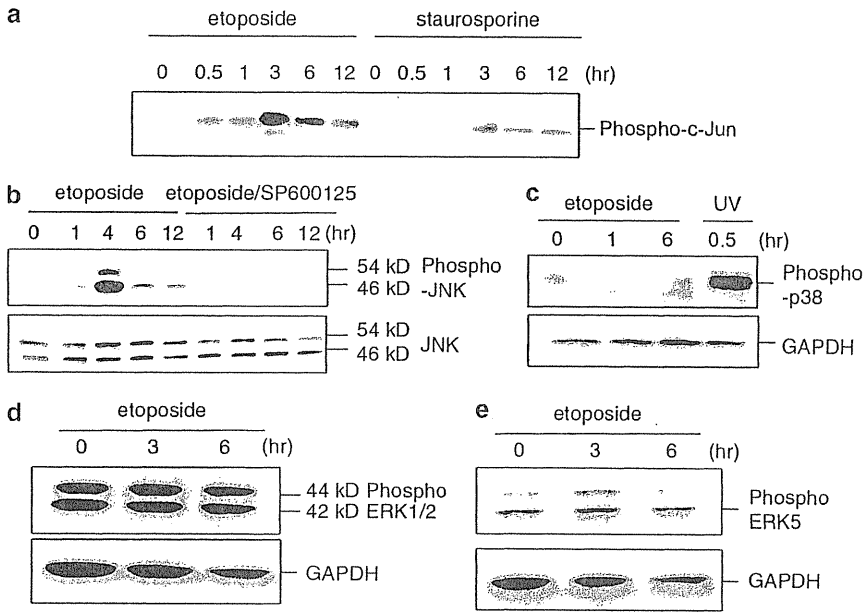

Figure 1 Phosphorylation of jun N-terminal kinase (JNK) after treatment of Bax/Bak double-knockout (DKO) mouse embryonic fibroblasts (MEFs) with etoposide or staurosporine. (**a**) DKO MEFs were treated with 20 μM etoposide or 1 μM staurosporine (STS) for the indicated periods. Cell lysates were subjected to an *in vitro* c-Jun kinase assay using an anti-phosphorylated c-Jun antibody. (**b**, **c**) DKO MEFs were treated with 20 μM etoposide or ultraviolet (UV) irradiation (100 J/m^2) in the presence or absence of 25 μM SP600125 for the indicated periods. Cell lysates were then subjected to immunoblot analysis with antibodies for phosphorylated JNK, JNK, phosphorylated p38 or glyceraldehyde 3-phosphate dehydrogenase (GAPDH; loading control). UV irradiation was used as a positive control for p38 activation. (**d**, **e**) DKO MEFs were treated with 20 μM etoposide for the indicated periods. Cell lysates were then subjected to immunoblot analysis with antibodies against phosphorylated extracellular ligand-regulated kinase (ERK)1/2, phosphorylated ERK5 or GAPDH (loading control).

Bcl-x_L die through an autophagic process after etoposide or staurosporine treatment (Shimizu *et al.*, 2004), Bcl-x_L was expressed in wild-type (WT) and sek1$^{-/-}$ mkk7$^{-/-}$ cells that were treated with etoposide. The WT cells overexpressing Bcl-x_L showed resistance to etoposide-induced cell death compared with vector-transfected WT MEFs, but still had a significant decline of viability, which was suppressed by the addition of 3-MA (Figure 3a). In contrast, the viability of Bcl-x_L-expressing sek1$^{-/-}$ mkk7$^{-/-}$ cells was higher than that of Bcl-x_L-expressing WT cells and was not influenced by the addition of 3-MA (Figure 3b). In both types of cells, the level of Bcl-x_L expression was equivalent and apoptosis was similarly inhibited (Figure 3c; data not shown). Therefore, 3-MA-sensitive autophagic cell death was blocked in Bcl-x_L-expressing sek1$^{-/-}$ mkk7$^{-/-}$ cells. Note that autophagy was activated similarly in both WT and sek1$^{-/-}$ mkk7$^{-/-}$ cells (Figure 3d). Consistent with the above findings, inhibition of autophagy using small interfering RNA (siRNA) for Atg5, which is essential for the induction of autophagy, improved the viability of Bcl-x_L-overexpressing WT cells, but not of Bcl-x_L-overexpressing sek1$^{-/-}$ mkk7$^{-/-}$ cells (Figures 3e and f). Thus, 3-MA-sensitive and Atg5-dependent autophagic cell death was induced in Bcl-x_L-overexpressing WT cells, but not in Bcl-x_L-overexpressing sek1$^{-/-}$ mkk7$^{-/-}$ cells, indicating that activation of JNK was required for the induction of autophagic cell death, consistent with the data shown in Figure 2.

JNK is activated during autophagic cell death, but not during starvation-induced autophagy

Autophagy occurs during autophagic cell death, but is also induced by starvation of cells. We have already demonstrated that JNK is activated during autophagic cell death. We next investigated whether starvation-induced autophagy was also accompanied by the activation of JNK. When Bax/Bak DKO MEFs were starved by incubation in Hanks solution, as described in Materials and methods section, autophagy occurred, as demonstrated by the punctate distribution of green fluorescent protein (GFP)-tagged light chain 3 (LC3; Figure 4a). As shown in Figure 4b, kinetics of autophagy induction were different between etoposide-treated cells and starved cells. Unlike etoposide treatment, starvation did not induce cell death (Figure 4c). As would be expected if it were assumed that autophagy was activated to promote survival during starvation, the death of these cells was enhanced by 3-MA (Figure 4c). In these cells, the level of JNK activation remained low compared with that in etoposide-treated cells (Figure 4d), suggesting that activation of JNK occurred with the induction of autophagic cell death but not autophagy for survival.

Co-activation of JNK and autophagy is sufficient to induce autophagic death of Bax/Bak DKO MEFs

Having shown that JNK has a crucial role in autophagic cell death, we next investigated whether JNK activation

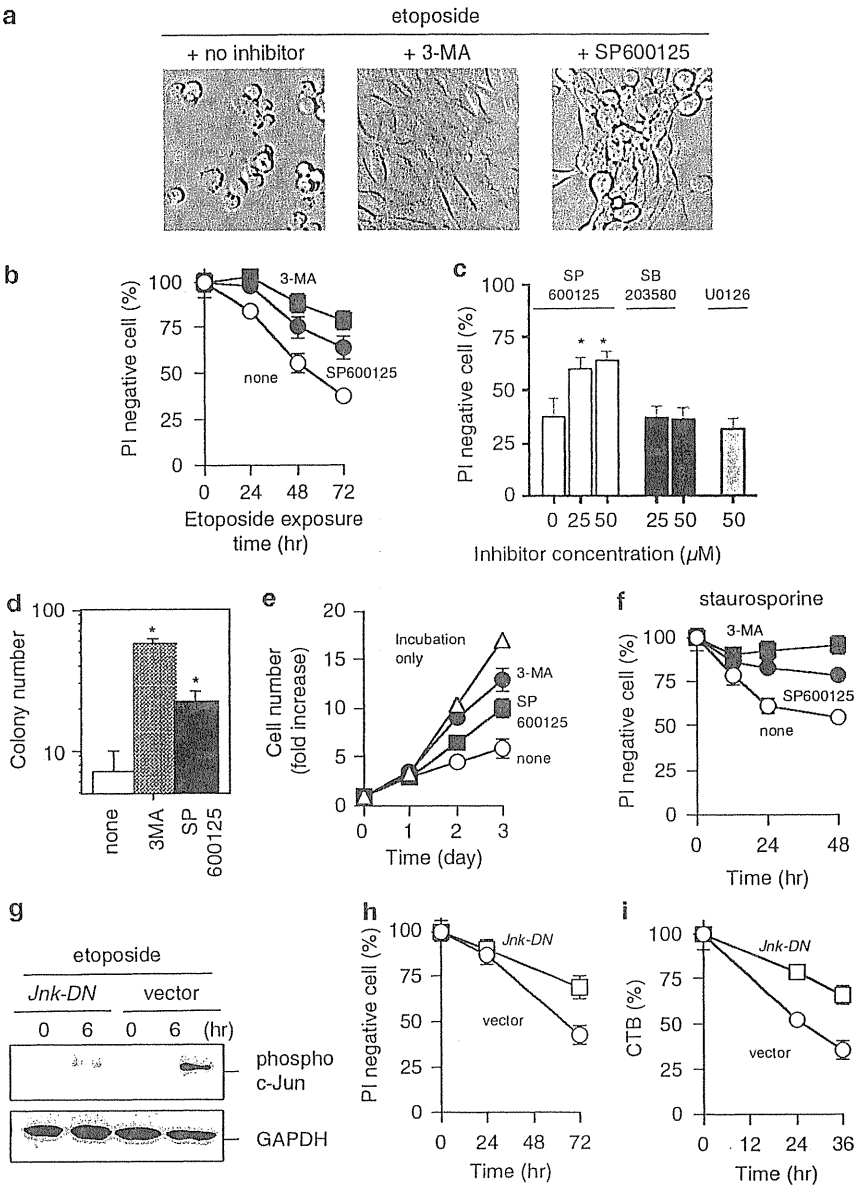

Figure 2 Reduction of etoposide-induced and staurosporine-induced death in Bax/Bak double-knockout (DKO) mouse embryonic fibroblasts (MEFs) by inhibition of jun N-terminal kinase (JNK). (**a**) DKO MEFs were treated with etoposide (20 μM) in the absence or presence of 10 mM 3-MA or 25 μM SP600125 for 24 h, and then were examined by phase-contrast microscopy. (**b**, **c**) Reduction of etoposide-induced autophagic cell death by SP600125 and 3-MA, but not SB203580 and U0126 as assessed by PI staining. (**b**) DKO MEFs were treated with 20 μM etoposide in the absence (open circles) or presence of 10 mM 3-MA (closed squares) or 25 μM SP600125 (closed circles) for the indicated periods. (**c**) DKO MEFs were treated with 20 μM etoposide in the presence of the indicated concentrations of SP600125, SB203580, or U0126 for 72 h. Cell viability was measured by staining with PI. Asterisks indicate a significant difference at $P<0.05$ (vs no inhibitor). (**d**, **e**) Reduction of etoposide-induced death by SP600125, as assessed by the clonogenic and proliferation assays. (**d**) DKO MEFs were treated with 20 μM etoposide in the absence or presence of 10 mM 3-methyl adenine (3-MA) or 25 μM SP600125 for 24 h. After collection, 2000 cells were seeded in normal medium and the number of colonies was counted after 1 week. Asterisks indicate a significant difference at $P<0.05$ (vs none). (**e**) DKO MEFs were untreated (open triangles) or treated with 20 μM etoposide in the absence (open circles) or presence of 10 mM 3-MA (closed circles) or 25 μM SP600125 (closed squares) for 24 h, and 5000 cells were seeded in normal medium. The number of viable cells was measured on the indicated days by the Cell Titer Blue (CTB) assay. (**f**) Reduction of staurosporine-induced autophagic cell death by SP600125 and 3-MA, as assessed by propidium iodide (PI) staining. DKO MEFs were treated with 1 μM staurosporine in the absence (open circles) or presence of 10 mM 3-MA (closed squares) or 25 μM SP600125 (closed circles) for the indicated periods. Cell viability was measured by PI staining. (**g–i**) Reduction of etoposide-induced autophagic cell death by a dominant-negative JNK mutation. DKO MEFs were transfected with plasmid DNA for the dominant-negative JNK mutation or the empty vector. After 24 h, cells were incubated with 20 μM etoposide for the indicated periods. Activation of JNK was assessed by the immunoblot analysis with antibodies for phsphorylated c-Jun (**g**). Cell viability was assessed by the PI staining (**h**) and CTB assay (**i**). In panels **b**–**f**, **h** and **i**, data are expressed as mean ± s.d. for four independent experiments.

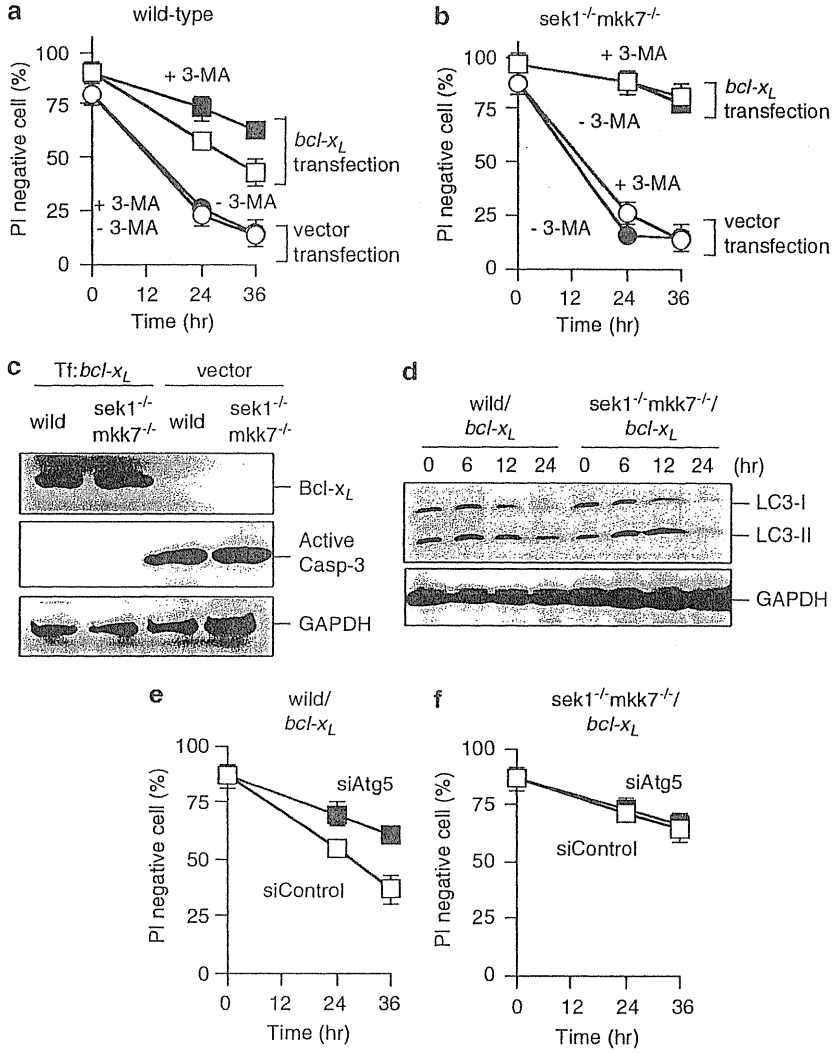

Figure 3 Suppression of etoposide-induced autophagic death in Bcl-x_L-overexpressing sek1$^{-/-}$mkk7$^{-/-}$ mouse embryonic fibroblast (MEF)-like cells. (**a**, **b**) Wild-type (**a**) and sek1$^{-/-}$mkk7$^{-/-}$ (**b**) MEF-like cells were transfected with plasmid DNA for Bcl-x_L (squares) or the empty vector (circles) for 24 h, and then were incubated with 20 μM etoposide in the presence (closed) or absence (open) of 10 mM 3-methyl adenine (3-MA) for the indicated periods. Cell viability was assessed by propidium iodide (PI) staining. Data are expressed as mean ± s.d. for four independent experiments. (**c**, **d**) Wild-type and sek1$^{-/-}$mkk7$^{-/-}$ MEF-like cells were transfected with plasmid DNA for Bcl-x_L or the empty vector, and then were incubated with 20 μM etoposide for 18 h (**c**) or for the indicated periods (**d**). Cell lysates were then subjected to immunoblot analysis with antibodies against Bcl-x_L or active caspases 3 (**c**) or light chain 3 (LC3) (**d**). Glyceraldehyde 3-phosphate dehydrogenase (GAPDH) is used as the loading control. (**e**, **f**) Wild-type (**e**) and sek1$^{-/-}$mkk7$^{-/-}$ (**f**) MEF-like cells were transfected with the Bcl-x_L expression plasmid together with Atg5 small interfering RNA (siRNA; closed squares) or control siRNA (open squares), and were incubated with 20 μM etoposide for the indicated periods. Cell viability was assessed by PI staining. Data are expressed as mean ± s.d. for four independent experiments.

was sufficient to induce autophagic cell death by using an MKK7–JNK fusion protein, in which MKK7α1 and JNK1β1 were connected by the Flag tag (Tsuruta *et al.*, 2004). Expression of this fusion protein led to constitutive activation of JNK through intramolecular phosphorylation by MKK7 (Figure 5a). As shown in Figure 5b, transient expression of MKK7–JNK in WT MEFs induced death, which was inhibited by zVAD-fmk. These findings indicated that WT MEFs underwent apoptosis due to autoactivation of JNK, consistent with numerous previous reports (Gupta *et al.*, 1995), thus verifying that MKK7–JNK functioned properly in our transfected cells. The addition of 3-MA enhanced this apoptosis, consistent with other report demonstrating that inhibition of autophagy enhances apoptosis (Boya *et al.*, 2005). We then introduced this plasmid into DKO MEFs. If activation of JNK was sufficient to induce autophagic cell death, expression of MKK7–JNK should have induced the death of Bax/Bak DKO MEFs. However, despite the similar level of JNK activation in WT and DKO MEFs (Figure 5a), expression of the MKK7–JNK fusion protein did not induce the death in Bax/Bak DKO MEFs (Figure 5b), indicating that activation of JNK alone was not sufficient to cause autophagic cell death.

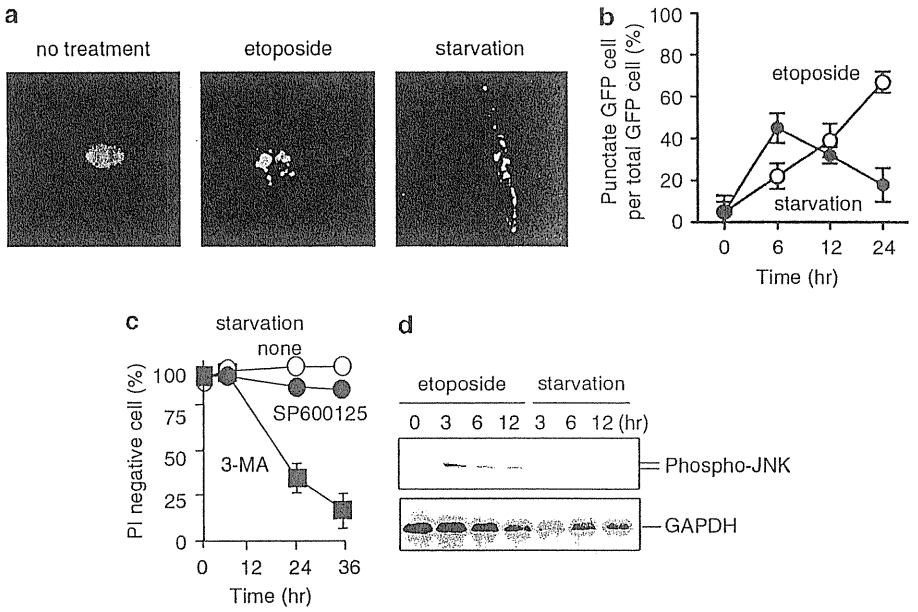

Figure 4 Jun N-terminal kinase (JNK) is not activated by starvation-induced autophagy. (**a**, **b**) Green fluorescent protein–light chain 3 (GFP–LC3)-transfected double-knockout (DKO) mouse embryonic fibroblasts (MEFs) were not treated, treated with 20 μM etoposide, or cultured in nutrient deprivation medium (starvation) for 12 h, and then were examined by fluorescent microscopy. (**a**) Representative photographs of cells showing GFP–LC3 are shown. (**b**) Time-course analysis of autophagic cells during starvation (closed circles) and etoposide treatment (open circles). Data are shown as mean ± s.d. ($n = 4$). (**c**) No autophagic death of starved DKO MEFs. DKO MEFs were cultured in nutrient deprivation medium in the absence (open circles) or presence of 10 mM 3-methyl adenine (3-MA; closed squares) or 25 μM SP600125 (closed circles). Cell viability was then measured by propidium iodide (PI) staining. Data are shown as mean ± s.d. ($n = 4$). (**d**) No activation of JNK by starvation. DKO MEFs were treated with 20 μM etoposide or were cultured in nutrient deprivation medium for the indicated periods. Cell lysates were subjected to immunoblot analysis with an antibody against phosphorylated JNK.

We next questioned whether the combination of autophagy and JNK activation could induce autophagic cell death. To elucidate this, we introduced MKK7–JNK plasmid into DKO MEFs and subjected to starvation. Although starvation or MKK7–JNK transfection alone did not induce cell death in DKO MEFs (Figures 4 and 5b), their combination significantly induced cell death that was greatly inhibited by 3-MA (Figure 5c), suggesting that co-activation of JNK and autophagy induced autophagic cell death.

JNK does not influence etoposide-induced autophagy in Bax/Bak DKO MEFs

As JNK activation was involved in etoposide- and staurosporine-induced autophagic death of Bax/Bak DKO MEFs, we next investigated whether JNK had an influence on autophagic process during the death of these cells. To examine this, GFP–LC3 was first expressed in Bax/Bak DKO MEFs. As a result, etoposide-treated Bax/Bak DKO MEFs showed punctate fluorescence due to the induction of autophagy (Figure 6a). This punctate fluorescence was inhibited by 3-MA, but not SP600125 (Figures 6a and b), although both agents inhibited autophagic cell death. Consistently, the majority of etoposide-treated DKO MEFs contained a number of autophagosomes/autolysosomes, observed with electron microscopy, irrespective of addition of the JNK inhibitor (Figure 6c). Similar results were also obtained using LC-3II formation (Figure 6d), which is a well-established indicator of autophagy (Kabeya *et al.*, 2000). Furthermore, accumulation of Beclin 1, a molecule involved in autophagy, was observed at similar levels in etoposide-treated DKO MEFs in the presence and absence of SP600125 (Figure 6d). Notably, the extent of etoposide-induced autophagy in Bcl-x_L-expressing $sek1^{-/-}$ $mkk7^{-/-}$ cells was the same as that in Bcl-x_L-expressing WT cells, as assessed by LC-3I/II generation (Figure 3d). All of these results indicated that inhibition of JNK suppressed autophagic cell death without affecting the occurrence of autophagy in etoposide-treated Bax/Bak DKO MEFs.

Activation of JNK occurs downstream of autophagy in etoposide-treated Bax/Bak DKO MEFs

Given that activation of JNK was involved in etoposide- and staurosporine-induced autophagic cell death, but not in the process of autophagy itself, we next investigated whether JNK activation occurred downstream of autophagy. We added 3-MA to etoposide-treated Bax/Bak DKO MEFs and then measured the phosphorylation of JNK. Inhibition of autophagy by 3-MA led to a marked reduction in the phosphorylation of JNK in etoposide-treated Bax/Bak DKO MEFs (Figure 7a), suggesting that the occurrence of autophagy was required for the activation of JNK. To confirm this, we used gene silencing with siRNA to inhibit Atg5. As shown in Figure 7b, silencing of Atg5 inhibited the

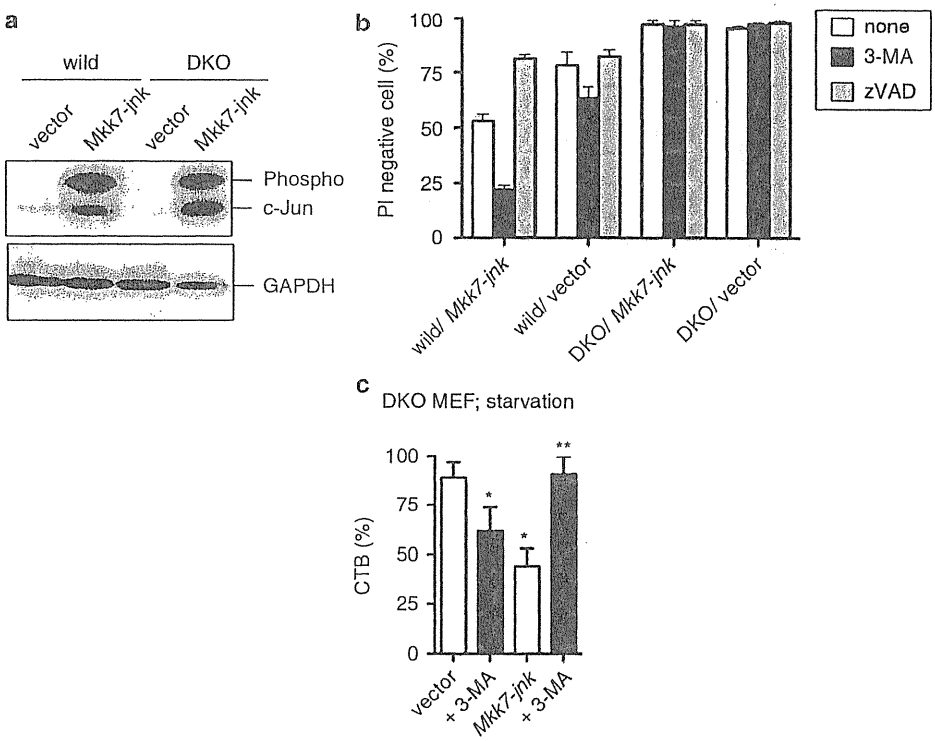

Figure 5 Enforced activation of jun N-terminal kinase (JNK) induced autophagic cell death in starved, but not healthy, Bax/Bak double-knockout (DKO) mouse embryonic fibroblasts (MEFs). (**a**) Wild-type and Bax/Bak DKO MEFs were transiently transfected with DNA encoding the *mkk7-jnk* fusion protein or empty vector for 24 h, and JNK activation was examined. Cell lysates were subjected to immunoblot analysis with an antibody against phosphorylated c-Jun. (**b**) Wild-type and Bax/Bak DKO MEFs were transiently transfected with DNA for the *mkk7-jnk* fusion protein or empty vector in the absence (white columns) or presence of 10 mM 3-methyl adenine (3-MA; black columns) or 100 μM benzyloxycarbonyl-Val-Ala-Asp (OMe) fluoromethylketone (zVAD-fmk; gray columns) for 24 h. Cell viability then was assessed by propidium iodide (PI) staining. Data are shown as mean ± s.d. ($n=4$). (**c**) Bax/Bak DKO MEFs were transiently transfected with the *mkk7-jnk* fusion plasmid or empty vector. After 24 h, cells were starved in the absence (white columns) or presence of 10 mM 3-MA (black columns) for 24 h. Cell viability then was assessed by Cell Titer Blue (CTB) assay. Data are shown as mean ± s.d. ($n=4$). Asterisks indicate significant differences at $P<0.05$ (*vs vector transfection only, **vs *mkk7-jnk* transfection only).

phosphorylation of JNK, similarly to the results obtained using 3-MA. Furthermore, as shown in Figure 7c, activation of JNK was not seen in Bcl-x_L-expressing Atg5$^{-/-}$ MEFs (Kuma *et al.*, 2004), whereas it was observed in Bcl-x_L-expressing Atg5$^{+/+}$ MEFs. The viability of Bcl-x_L-expressing Atg5$^{-/-}$ MEFs was superior to that of Bcl-x_L-expressing Atg5$^{+/+}$ MEFs in response to etoposide, despite the equivalent expression levels of Bcl-x_L (Figure 7d). Therefore, these results indicated that the activation of JNK occurred downstream of the induction of autophagy, and that JNK activation then induced cell death.

Activation of JNK induces autophagic cell death in Bcl-x_L-overexpressing HeLa cells

Finally, we questioned whether JNK-mediated autophagic cell death also occurred in apoptosis-resistant human cancer cells. To examine this, we produced apoptosis-resistant HeLa cells by stably overexpressing Bcl-x_L (designated as HeLa/Bcl-x_L; Figure 8a). In contrast to the etoposide-treated Bax/Bak DKO MEFs, which did not die by apoptosis but lost their viability by autophagic cell death (Figure 2b), HeLa/Bcl-x_L cells maintained their viability in the presence of etoposide (Figure 8b). To elucidate a reason why HeLa/Bcl-x_L cells could avoid the autophagic cell death, we examined the induction of autophagy and JNK activation. Induction of autophagy was observed in etoposide-treated HeLa/Bcl-x_L cells, as assessed by GFP–LC3 (Figure 8d) and LC3-II generation (Figure 8e). In contrast, etoposide-induced JNK activation in Hela/Bcl-x_L cells was much weaker than that in etoposide-treated DKO MEFs (Figure 8f). Therefore, we hypothesized that the lower levels of JNK activation in Hela/Bcl-x_L cells was responsible for their resistance to autophagic cell death. To examine this possibility, we introduced *mkk7-jnk* expression plasmid into HeLa/Bcl-x_L cells (Figure 8c) and treated the cells with etoposide. In response to etoposide, *mkk7-jnk*-transfected HeLa/Bcl-x_L cells showed autophagy induction (Figures 8d and e) and lost their viability, which was inhibited by 3-MA (Figure 8g), suggesting the occurrence of autophagic cell death. Taken together, co-activation of autophagy and JNK is crucial for the induction of autophagic cell death.

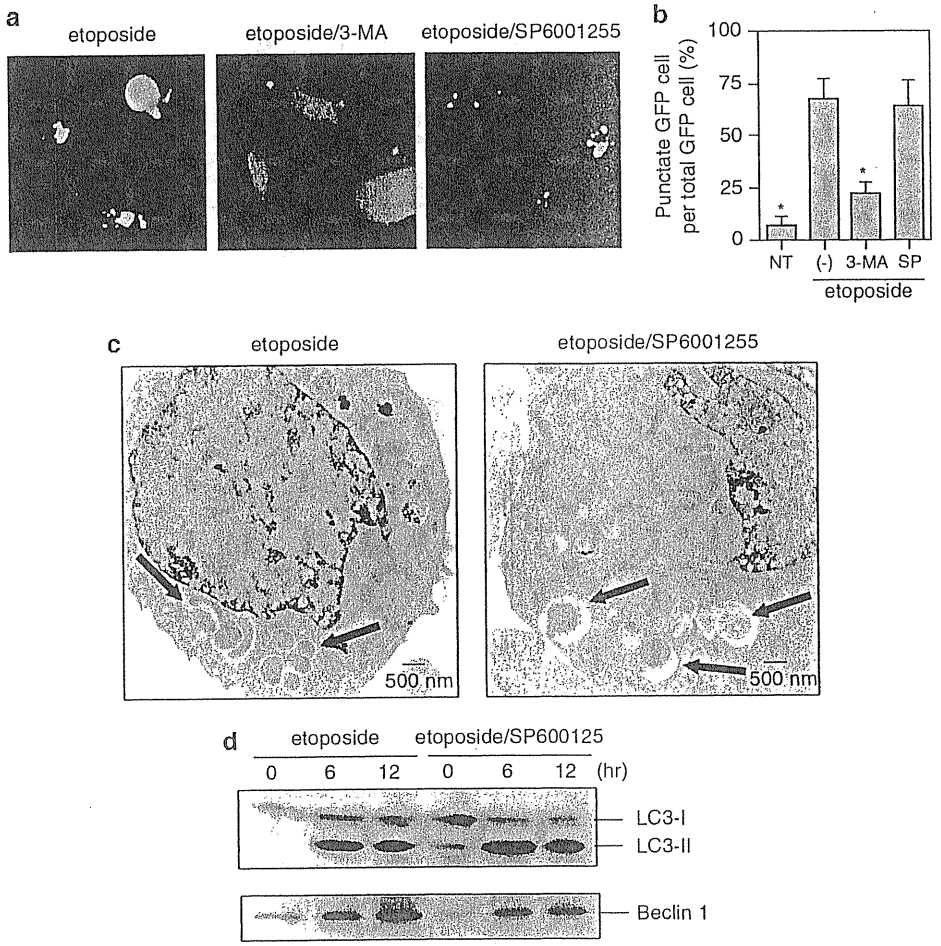

Figure 6 No effect of a jun N-terminal kinase (JNK) inhibitor on etoposide-induced autophagy of Bax/Bak double-knockout (DKO) mouse embryonic fibroblasts (MEFs). (**a**, **b**) Green fluorescent protein–light chain 3 (GFP–LC3)-transfected DKO MEFs were treated with 20 μM etoposide in the absence or presence of 25 μM SP600125 (SP) or 10 mM 3-methyl adenine (3-MA) for 24 h, and then were examined by fluorescent microscopy. Representative photographs are shown in (**a**), and the percentage of cells with punctate GFP relative to all GFP-positive cells is indicated in (**b**). Data are shown as mean ± s.d. ($n=4$). Asterisks indicate a significant difference at $P<0.05$ (vs etoposide only). (**c**) Representative electron micrograph of Bax/Bak DKO MEFs treated with etoposide for 18 h in the presence or absence of SP600125. Arrows indicate autophagosomes/autolysosmes. (**d**) DKO MEFs were treated with 20 μM etoposide in the absence or presence of 25 μM SP600125 for the indicated periods. Then cell lysates were subjected to immunoblot analysis with an antibody against LC3 and Beclin 1.

Discussion

Autophagic cell death is thought to be involved in various physiological and pathological events. However, it has long been assessed only from the point of view of morphological changes due to lack of knowledge regarding the molecular events involved in this process, making it difficult to fully understand the role of autophagic cell death *in vivo*. Recently, Lenardo and colleagues and our group reported different experimental systems, in which autophagic cell death could be activated, which were suitable for investigating the molecular mechanisms of autophagic cell death (Shimizu *et al.*, 2004; Yu *et al.*, 2004). Although the two cellular systems are different, they may share the core machinery of autophagic cell death. Lenardo and colleagues reported that caspase-8, JNK and degradation of catalase were involved in the autophagic death of zVAD-fmk-treated L929 cells (Yu *et al.*, 2004, 2006). Our preliminary studies excluded the involvement of caspase-8 and catalase in the autophagic death of Bax/Bak DKO cells, as the extent of autophagic cell death was equal in Bcl-x_L-overexpressing caspase-8-deficient MEFs and Bcl-x_L-overexpressing wild-type MEFs after etoposide stimulation (Shimizu, unpublished data), and as significant degradation of catalase was not observed in etoposide-treated Bax/Bak DKO MEFs (Shimizu, unpublished data). In contrast, involvement of JNK seems to be common to both of these autophagic cell death systems. This study showed that: (1) JNK is activated when autophagic cell death is induced in Bax/Bak DKO MEFs by etoposide and staurosporine, but not when cells are starved; (2) autophagic cell death is suppressed by inhibition of JNK; (3) activation of JNK is required (but not sufficient) for autophagic cell death; and (4) activation of JNK is largely dependent on the

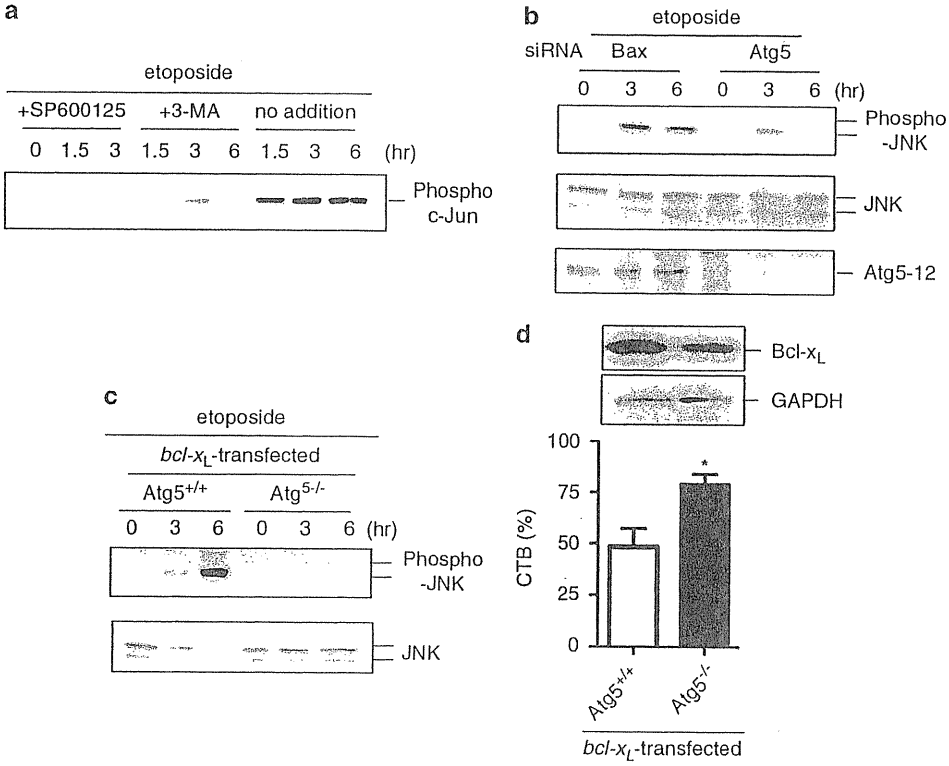

Figure 7 Involvement of autophagy in etoposide-induced activation of JNK in double-knockout (DKO) mouse embryonic fibroblasts (MEFs). (**a**) DKO MEFs were treated with 20 μM etoposide in the absence or presence of 25 μM SP600125 or 10 mM 3-methyl adenine (3-MA) for the indicated periods. Cell lysates were subjected to an *in vitro* c-Jun kinase assay by western blotting using an anti-phosphorylated c-Jun antibody. (**b**) DKO MEFs were treated with the indicated small interfering RNAs (siRNAs) for 24 h and then incubated with 20 μM etoposide for the indicated periods. Cell lysates were subjected to western blotting with anti-phosphorylated JNK, anti-JNK and anti-Atg5 (Atg5-12) antibodies. (**c**, **d**) $Atg5^{+/+}$ and $Atg5^{-/-}$ MEFs were transfected with the *bcl-x*$_L$ complementary DNA for 24 h and then incubated with 20 μM etoposide for the indicated periods. Cell lysates were subjected to western blotting with anti-phosphorylated JNK antibodies, anti-JNK antibodies (**c**) and Bcl-x_L (**d**). Glyceraldehyde 3-phosphate dehydrogenase (GAPDH) is used as a loading control. Cell viability was assessed by the Cell Titer Blue (CTB) assay (**d**). Data are shown as mean ± s.d. ($n = 4$). Asterisks indicate a significant difference at $P < 0.05$.

autophagic process. These results indicate that JNK is involved in autophagic cell death without influencing the process of autophagy itself, which could be an important piece of information regarding the molecular mechanisms of autophagic cell death.

Jun N-terminal kinase belongs to the mitogen-activated protein kinases and is activated by apoptosis signal-regulating kinase 1 (mitogen-activated protein kinase kinase kinase) and SEK1/MKK7 (mitogen-activated protein kinase kinase) when cells are exposed to various stresses (Davis, 2000). The role of JNK in cell death has long been studied. The activation of JNK is observed when apoptosis is induced by various stressors, including ultraviolet irradiation and tumor necrosis factor, but its function has long been controversial, as it has a pro-apoptotic role in some physiological and pathological conditions, whereas it exerts an anti-apoptotic effect in other situations (Davis, 2000). However, at least, part of this complex issue has been explained by the discovery of different modes of JNK activation (Ventura *et al.*, 2006). The early transient phase of JNK activation signals for cell survival, whereas sustained JNK activation can trigger apoptotic signals. Sustained activation of JNK has also been reported to mediate reactive oxygen species-induced necrosis (Nakano *et al.*, 2006). Similarly, we observed the sustained activation of JNK for more than 6 h (Figure 1) in Bax/Bak DKO MEFs undergoing etoposide-induced autophagic cell death. Therefore, sustained JNK activation seems to be harmful for cells.

How does sustained JNK activation induce cell death? In the case of necrosis, JNK has been reported to act as a positive regulator of reactive oxygen species production (Nakano *et al.*, 2006), although the precise mechanisms involved are unclear. The mechanisms that account for pro-apoptotic signaling by JNK have been studied extensively, and various downstream molecules have been proposed. In neurons, especially in developing neurons, JNK induces apoptosis by activating c-jun-mediated transcription (Behrens *et al.*, 1999). In other cells, however, JNK-mediated apoptosis does not require *de novo* protein synthesis because direct phosphorylation of target molecules induces apoptosis (Tournier *et al.*, 2000). In any case, JNK functions upstream of apoptotic mitochondrial changes, so that the absence of Bax and Bak blocks JNK-mediated apoptosis. This was confirmed

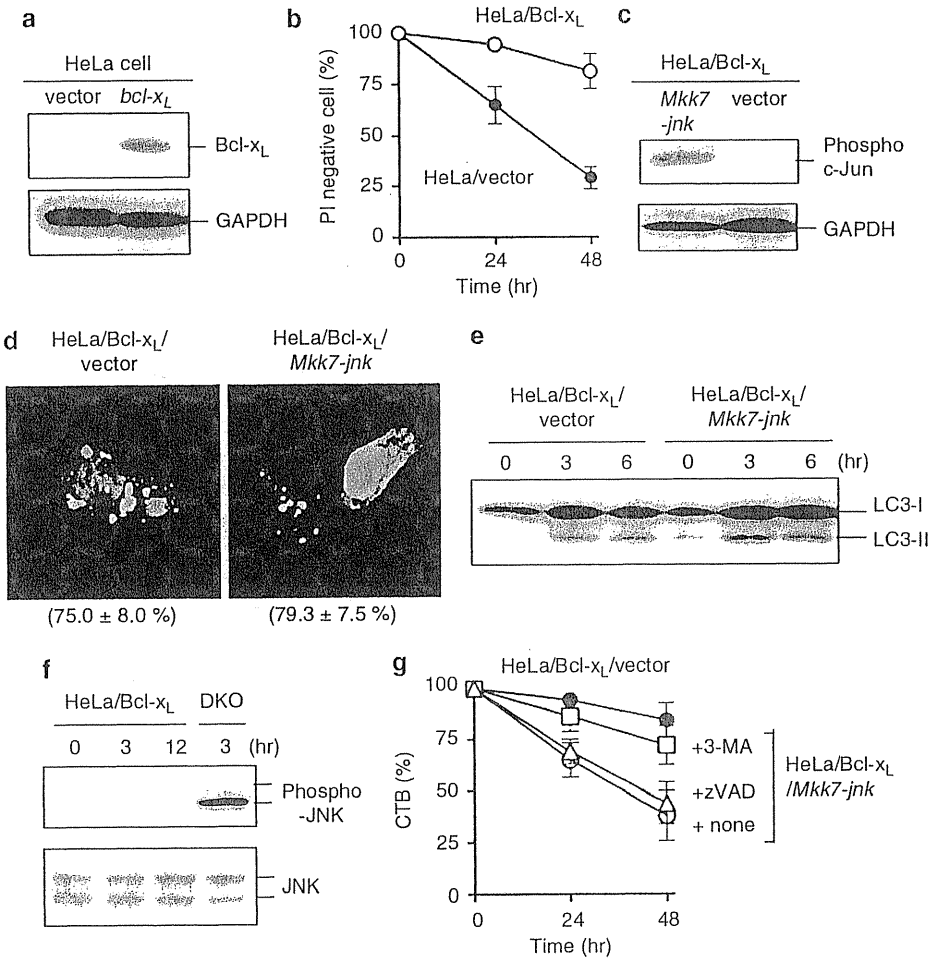

Figure 8 Induction of autophagic cell death in HeLa/Bcl-xL cells by co-activation of jun N-terminal kinase (JNK) and autophagy. (**a**, **b**) HeLa cells were stably transfected with the human *bcl-x*$_L$ plasmid or empty vector. Cell lysates were subjected to immunoblot analysis with an antibody against human Bcl-x$_L$ (**a**). Cells were treated with 100 μM etoposide for the indicated hours and viability was assessed by propidium iodide (PI) staining (**b**). Data are shown as mean ± s.d. ($n = 4$). (**c**) HeLa/Bcl-x$_L$ cells were transiently transfected with DNA for the *mkk7-jnk* fusion protein or empty vector for 24 h, and JNK activation was examined. Cell lysates were subjected to immunoblot analysis with an antibody against phosphorylated c-Jun. (**d**, **e**) HeLa/Bcl-x$_L$ cells were transiently transfected with DNA for the *mkk7-jnk* fusion protein or empty vector together with green fluorescent protein–light chain 3 (GFP–LC3) plasmid for 24 h, then cells were treated with 100 μM etoposide for 6 h. (**d**) Representative photographs and the percentage of cells with punctate GFP relative to all GFP-positive cells are shown. Data are shown as mean ± s.d. ($n = 4$). (**e**) Cell lysates were subjected to immunoblot analysis with an antibody against LC3. (**f**) Weak activation of JNK in etoposide-treated HeLa/Bcl-x$_L$ cells. HeLa/Bcl-x$_L$ cells were treated with 100 μM etoposide for the indicated periods. Cell lysates were subjected to immunoblot analysis with an antibody against phosphorylated JNK and JNK. As a positive control, lysates from Bax/Bak double-knockout (DKO) mouse embryonic fibroblasts (MEFs) treated with 20 μM etoposide for 3 h were used. These antibodies equivalently cross-react with human and mouse proteins. (**g**) HeLa/Bcl-x$_L$ cells were transiently transfected with DNA for the *mkk7-jnk* fusion protein (open symbols) or empty vector (closed symbols) for 24 h, then cells were treated with 100 μM etoposide in the absence (circles) or presence of 10 mM 3-MA (squares) or 100 μM benzyloxycarbonyl-Val-Ala-Asp (OMe) fluoromethylketone (zVAD-fmk; triangles) for 48 h. Cell viability was assessed by Cell Titer Blue (CTB) assay. Data are shown as mean ± s.d. ($n = 4$).

by our findings that over-activation of JNK induced the apoptosis of wild-type MEFs, but not of Bax/Bak DKO MEFs (Figure 5). These data also suggested the possibility that Bcl-2 family members could be direct target(s) of JNK. Actually, JNK induces the expression of BH3-only proteins: Hrk and Bim (Harris and Johnson, 2001). Jun N-terminal kinase also phosphorylates Bcl-2 family members and promotes pro-apoptotic Bax activity (Kim *et al.*, 2006), and inhibits various anti-apoptotic Bcl-2 family members, including Bcl-2, Bcl-x$_L$ and Mcl-1 (Ito *et al.*, 1997; Park *et al.*, 1997). In addition, JNK indirectly determines the activation of Bax through its regulation of 14-3-3 (Tsuruta *et al.*, 2004). Thus, the Bcl-2 family proteins are considered to be likely targets of JNK during the process of apoptosis. With regard to autophagic cell death, we have previously reported that Bcl-x$_L$ may regulate the autophagic death of etoposide-treated DKO MEFs (Shimizu *et al.*, 2004), so this molecule might be a target when JNK activates autophagic cell death.

The molecular mechanism of JNK activation is another crucial issue with regard to understanding

autophagic cell death. We found several pieces of evidence that suggest that the activation of JNK largely occurs in an autophagy-dependent manner: (1) 3-MA-mediated inhibition of autophagy suppressed JNK activation (Figure 7a), (2) silencing of the *Atg5* gene also suppressed JNK activation (Figure 7b), and (3) JNK activation was weaker in Bcl-x_L-overexpressing $Atg5^{-/-}$ MEFs than in Bcl-x_L-overexpressing $Atg5^{+/+}$ MEFs (Figure 7c). These results indicate that activation of the autophagic process can activate JNK, but induction of autophagy does not necessarily lead to JNK activation. Whether autophagy activates JNK seems to depend on the stimulus, as etoposide and staurosporine, but not starvation, induced JNK activation as shown in this study. Why does JNK activation occur during etoposide/staurosporine-induced autophagic cell death, but not during starvation, although autophagy is activated in both cases? There are two possibilities that can be suggested. We have previously shown that some autophagic proteins, including Atg5 and Beclin 1, are upregulated during etoposide/staurosporine-induced autophagic cell death, but not during starvation (Shimizu *et al.*, 2004). Therefore, a difference in the level of autophagic activity may determine whether JNK activation occurs. Alternatively, other signals in addition to autophagy itself might be required for the activation of JNK. In any case, autophagy may activate endoplasmic reticulum stress or oxidative stress during digestion of endoplasmic reticulum or mitochondria, which may activate JNK signaling pathway.

In contrast to our findings, several investigators have described that JNK activation occurred upstream of the induction of autophagy or autophagic cell death when various cells are starved (Wei *et al.*, 2008), treated with tumor necrosis factor (Cheng *et al.*, 2008) and ceramide (Li *et al.*, 2009). Possible explanation for this discrepancy might be the difference of the cell types or stimuli used. Tumor necrosis factor and oxidative stress directly activate JNK through tumor necrosis factor receptor-associated factor 2 and apoptosis signal-regulating kinase 1, respectively. In contrast, other signals, such as etoposide, could not directly activate JNK. In such case, JNK activation may be dependent on the environmental and genetic circumstances. Further studies will be necessary to address this issue.

Materials and methods

Antibodies and chemicals

Anti-phospho c-Jun (Ser63)II, anti-stress-activated protein kinase/JNK, anti-phospho p38, anti-phospho stress-activated protein kinase/JNK (Thr183/Tyr185), anti-phospho ERK1/2 and anti-phospho ERK5 antibodies were obtained from Cell Signaling Technologies (Danvers, MA, USA). Anti-Bcl-x_L (S-18), anti-active caspase-3 and anti-LC3 polyclonal antibodies were purchased from Santa Cruz Biotechnology (Santa Cruz, CA, USA), Promega (Madison, WI, USA) and MBL (Nagoya, Japan), respectively. A stress-activated protein kinase/JNK Kinase Assay Kit (nonradioactive) was purchased from Cell Signaling Technologies. The inhibitors SP600125 and SB203580 were obtained from Tocris Bioscience (Ellisville, MO, USA). Cell Titer Blue and 3-MA were purchased from ICN Biochemicals (Irvine, CA, USA) and Promega, respectively. Other chemicals were purchased from Wako (Osaka, Japan).

Cell culture and DNA transfection

$Bax^{-/-}Bak^{-/-}$ (DKO), $Atg5^{-/-}$ and $Atg5^{+/+}$ MEFs were collected from mouse embryos at E14.5, and immortalized with Simian virus 40 T antigen (Shimizu *et al.*, 2004). Mouse embryonic fibroblasts were cultured in Dulbecco's modified Eagle's medium supplemented with 2 mM L-glutamine, 1 mM sodium pyruvate, 0.1 mM non-essential amino acids, 10 mM HEPES/Na^+, (pH 7.4), 0.05 mM 2-mercaptoethanol, 100 U/ml penicillin, 100 μg/ml streptomycin and 10% fetal bovine serum. Sek1/MKK7 double-knockout embryonic stem cells were used as MEF-like cells, and were cultured as described previously (Nishitai *et al.*, 2004). For starvation of cells, culturing was done in Hanks' balanced salt solution supplemented with 1 mM sodium pyruvate, 10 mM HEPES/Na^+ (pH 7.4) and 0.05 mM 2-mercaptoethanol. HeLa/Bcl-x_L cells were generated by transfection of the expression plasmid for human Bcl-x_L.

The plasmids pCMV5-JNK1 APF (the mammalian expression plasmid for dominant-negative JNK; Gupta *et al.*, 1995), pCDNA3 MKK7-JNK1 WT (the mammalian expression plasmid for the MKK7–JNK1 fusion gene; Gupta *et al.*, 1995) and pCAGGS-GFP-LC3 (Kabeya *et al.*, 2000) were kindly provided by Drs R Davis, Y Gotoh and N Mizushima, respectively. The pUC-CAGGS expression vector with DNA encoding human Bcl-x_L has been described earlier (Shimizu *et al.*, 1996). Cells (1×10^6) were transfected with plasmid DNA using the Amaxa electroporation system according to the supplier's protocol (kit V, program U-20). The transfection efficiency was more than 75%, as assessed by co-transfection with DNA expressing GFP. All siRNAs were produced by Dharmacon Research. The sequences used are as follows (numbers in parentheses indicate nucleotide positions within the respective open reading frames): mouse Atg5 siRNA: 5′-AACUUGCUUUACUCUCUAUCA-3′ (51–71). Cells (1×10^6) were transfected with 10 μg of siRNA using the Amaxa electroporation system.

Analysis of mitogen-activated protein kinase activation

Cells were seeded into 6-well dishes at a density of 3.5×10^6 cells per well. After 24 h, cells were treated with etoposide (20 μM), staurosporine (1 μM), ultraviolet irradiation (100 J/m^2), or were nutrient deprived in the presence or absence of SP600125 (25 μM) and 3-MA (10 mM). The *in vitro* kinase assay was performed according to the supplier's protocol. Briefly, cell lysates were mixed with c-Jun fusion protein-coated agarose beads at 4 °C for 12 h. After centrifugation and washing, beads were suspended in the Kinase Buffer supplemented with 200 mM ATP for 30 min at 30 °C. Then phosphorylated c-Jun was detected with an anti-phospho-c-Jun antibody. The activation of JNK was also evaluated by western blotting using an anti-phospho JNK monoclonal antibody. The activation of p38, ERK1/2 and ERK5 was assessed by western blotting.

Cell viability assay

Cells were seeded into 6-well dishes at a density of 3.5×10^6 cells per well. After 24 h, cells were exposed to etoposide (20 μM), staurosporine (1 μM) or were nutrient deprived in the presence or absence of SP600125, SB203580, 3-MA or z-VAD-fmk at the indicated concentrations. Cells, including floating cells, were then collected and viability was assessed by propidium iodide (PI) staining or CTB assay (Shimizu *et al.*,

2004). Briefly, cells were stained with 1 μM PI for 5 min at room temperature, and then were analyzed using a flow cytometer (FACS Caliber; Becton-Dickinson, Franklin Lakes, NJ, USA). The CTB assay was carried out using Cell Titer Blue assay reagent according to the supplier's protocol.

To examine proliferative activity, MEFs were treated with etoposide, all the cells were recovered, and then, 5000 or 10 000 cells were re-cultured in standard medium in 96-well or 48-well dishes, respectively. Viable cells were measured on the indicated days by the CTB assay (Shimizu *et al.*, 2004). For the colony formation assay, MEFs were treated with etoposide, collected and 2000 cells were seeded into 24-well dishes containing standard medium. After 1 week, the number of colonies was counted (Shimizu *et al.*, 2004).

Western blot analysis

Whole-cell protein extracts were prepared using RIPA buffer, and the protein content was quantified by Lowry's method (Bio-Rad, Tokyo, Japan) according to the manufacturer's instructions. Proteins were then separated by electrophoresis on 15% sodium dodecyl sulfate–polyacrylamide gels and transferred to polyvinylidene fluoride membranes. Filters were treated with the indicated antibodies and proteins were detected using the appropriate horseradish peroxidase-conjugated secondary antibodies and enhanced chemiluminescent reagent (GE healthcare Japan, Tokyo, Japan).

Staining of autophagosomes and lysosomes/autolysosomes

Cells were transfected with 1 μg of GFP–LC3 expression plasmid (Kabeya *et al.*, 2000). After 24 h, cells were subjected to etoposide treatment or starvation and GFP–LC3 fluorescence was observed under a confocal fluorescence microscope (LSM 510 META, Zeiss Japan, Tokyo, Japan).

Electron microscopy

Cells were fixed with 2% paraformaldehyde/2% glutaraldehyde in 0.1 M phosphate buffer (pH 7.4), followed by fixing in 1% OsO_4. After dehydration, ultrathin sections were stained with uranyl acetate and lead citrate for observation under a JEM 100 CX electron microscope (JEOL, Tokyo, Japan).

Conflict of interest

The authors declare no conflict of interest.

Acknowledgements

We thank Dr N Mizushima for providing us with MEFs from $Atg5^{-/-}$ and $Atg5^{+/+}$ mice and pCAGGS-GFP-LC3 plasmid. We also thank Drs R Davis and Y Gotoh for providing PCMV5-JNK1 APF plasmid and pCDNA3 MKK7-JNK1 WT plasmid, respectively. This study was partly supported by the Program for Promotion of Fundamental Studies in Health Sciences of the National Institute of Biomedical Innovation (NIBIO); a grant for Scientific Research on Priority Areas, SORST of Japan Science and Technology Corp; a grant for the 21st Century COE Program; a grant for Creative Scientific Research from the Japanese Ministry of Education, Science, Sports and Culture; and a grant for Comprehensive Research on Aging and Health from the Japanese Ministry of Health, Labor and Welfare. This study was also supported by grants from the Uehara Memorial Foundation and the Naito Foundation.

References

Bachrecke EH. (2002). How death shapes life during development. *Nat Rev Mol Cell Biol* **3**: 779–787.

Behrens A, Sibilia M, Wagner FF. (1999). Amino-terminal phosphorylation of c-Jun regulates stress-induced apoptosis and cellular proliferation. *Nat Genet* **21**: 326–329.

Boya P, Gonzalez-Polo RA, Casares N, Perfettini JL, Dessen P, Larochette N *et al.* (2005). Inhibition of macroautophagy triggers apoptosis. *Mol Cell Biol* **25**: 1025–1040.

Cheng Y, Qiu F, Tashiro S, Onodera S, Ikejima T. (2008). ERK and JNK mediate TNFalpha-induced p53 activation in apoptotic and autophagic L929 cell death. *Biochem Biophys Res Commun* **376**: 483–488.

Clarke PG. (1990). Developmental cell death: morphological diversity and multiple mechanisms. *Anat Embryol (Berl)* **181**: 195–213.

Davis RJ. (2000). Signal transduction by the JNK group of MAP kinases. *Cell* **103**: 239–252.

Gupta S, Campbell D, Derijard B, Davis RJ. (1995). Transcription factor ATF2 regulation by the JNK signal transduction pathway. *Science* **267**: 389–393.

Harris CA, Johnson Jr EM. (2001). BH3-only Bcl-2 family members are coordinately regulated by the JNK pathway and require Bax to induce apoptosis in neurons. *J Biol Chem* **276**: 37754–37760.

Ito T, Deng X, Carr B, May WS. (1997). Bcl-2 phosphorylation required for anti-apoptosis function. *J Biol Chem* **272**: 11671–11673.

Kabeya Y, Mizushima N, Ueno T, Yamamoto A, Kirisako T, Noda T *et al.* (2000). LC3, a mammalian homologue of yeast Apg8p, is localized in autophagosome membranes after processing. *EMBO J* **19**: 5720–5728.

Kim BJ, Ryu SW, Song BJ. (2006). JNK- and p38 kinase-mediated phosphorylation of Bax leads to its activation and mitochondrial translocation and to apoptosis of human hepatoma HepG2 cells. *J Biol Chem* **281**: 21256–21265.

Klionsky DJ. (2005). Autophagy. *Curr Biol* **15**: R282–R283.

Kuma A, Hatano M, Matsui M, Yamamoto A, Nakaya H, Yoshimori T *et al.* (2004). The role of autophagy during the early neonatal starvation period. *Nature* **432**: 1032–1036.

Levine B, Yuan J. (2005). Autophagy in cell death: an innocent convict? *J Clin Invest* **115**: 2679–2688.

Li DD, Wang LL, Deng R, Tang J, Shen Y, Guo JF *et al.* (2009). The pivotal role of c-Jun NH2-terminal kinase-mediated Beclin 1 expression during anticancer agents-induced autophagy in cancer cells. *Oncogene* **28**: 886–898.

Mizushima N, Ohsumi Y, Yoshimiri T. (2002). Autophagosome formation in mammalian cells. *Cell Struct Funct* **6**: 421–429.

Nakano H, Nakajima A, Sakon-Komazawa S, Piao JH, Xue X, Okumura K. (2006). Reactive oxygen species mediate crosstalk between NF-kappaB and JNK. *Cell Death Differ* **5**: 730–737.

Nishitai G, Shimizu N, Negishi T, Kishimoto H, Nakagawa K, Kitagawa D *et al.* (2004). Stress induces mitochondria-mediated apoptosis independent of SAPK/JNK activation in embryonic stem cells. *J Biol Chem* **279**: 1621–1626.

Ohsumi Y. (2001). Molecular dissection of autophagy: two ubiquitin-like systems. *Nat Rev Mol Cell Biol* **2**: 211–216.

Park J, Kim I, Oh YJ, Lee K, Han PL, Choi EJ. (1997). Activation of c-Jun N-terminal kinase antagonizes an anti-apoptotic action of Bcl-2. *J Biol Chem* **272**: 16725–16728.

Shimizu S, Eguchi Y, Kamiike W, Matsuda H, Tsujimoto Y. (1996). Bcl-2 expression prevents activation of the ICE protease cascade. *Oncogene* **12**: 2251–2257.

Shimizu S, Kaneseki T, Mizushima N, Mizuta K, Arakawa-Kobayashi S, Thompson CB *et al.* (2004). Role of Bcl-2 family proteins in a non-apoptotic programmed cell death dependent on autophagy genes. *Nat Cell Biol* **6**: 1221–1228.

Tournier C, Hess P, Yang DD, Xu J, Turner TK, Nimnual A *et al.* (2000). Requirement of JNK for stress-induced activation of the cytochrome *c*-mediated death pathway. *Science* **88**: 870–874.

Tsuruta F, Sunayama J, Mori Y, Hattori S, Shimizu S, Tsujimoto Y *et al.* (2004). JNK promotes Bax translocation to mitochondria through phosphorylation of 14-3-3 proteins. *EMBO J* **23**: 1889–1899.

Ventura JJ, Hubner A, Zhang C, Flavell RA, Shokat KM, Davis RJ. (2006). Chemical genetic analysis of the time course of signal transduction by JNK. *Mol Cell* **21**: 701–710.

Yu L, Alva A, Su H, Dutt P, Freundt E, Welsh S *et al.* (2004). Regulation of an ATG7-beclin 1 program of autophagic cell death by caspase-8. *Science* **304**: 1500–1502.

Yu L, Wan F, Dutta S, Welsh S, Liu Z, Freundt E *et al.* (2006). Autophagic programmed cell death by selective catalase degradation. *Proc Natl Acad Sci USA* **103**: 4952–4957.

Wei Y, Pattingre S, Sinha S, Bassik M, Levine B. (2008). JNK1-mediated phosphorylation of Bcl-2 regulates starvation-induced autophagy. *Mol Cell* **30**: 678–688.

Laboratory Investigation (2010) 90, 1357–1364

Mice lacking Dok-1, Dok-2, and Dok-3 succumb to aggressive histiocytic sarcoma

Ryuichi Mashima[1], Kazuho Honda[2], Yi Yang[3], Yohei Morita[4], Akane Inoue[1], Sumimasa Arimura[1], Hiroshi Nishina[5], Hideo Ema[4], Hiromitsu Nakauchi[4], Brian Seed[6], Hideaki Oda[2] and Yuji Yamanashi[1]

Histiocytic sarcoma (HS), a rare hematological malignancy, is an aggressive neoplasm that responds poorly to therapy. The molecular etiology and pathology of this disease remain unclear, hampering the development of an effective therapy, and there remains a need for more, and more realistic, animal models. HS cells typically show a histiocytic (ie, tissue macrophage-like) morphology and express histiocyte/macrophage markers in the absence of lymphocyte markers. In this study, we report that *Dok-1*$^{-/-}$*Dok-2*$^{-/-}$*Dok-3*$^{-/-}$ mice develop HS, but do not exhibit elevated incidence of other types of tumors. These mutant mice showed earlier mortality than wild-type (WT) or the other mutant mice, and this mortality was associated with HS. In total, 17 of 21 tumor-bearing *Dok-1*$^{-/-}$*Dok-2*$^{-/-}$*Dok-3*$^{-/-}$ mice necropsied at 25–66 weeks of age showed multiple organ spread, with osteolytic lesions and orthotopic invasion from the bone marrow to skeletal muscle. Tumors from the mice were transplantable. In addition, all *Dok-1*$^{-/-}$*Dok-2*$^{-/-}$*Dok-3*$^{-/-}$ mice, but only a small proportion of *Dok-3*$^{-/-}$ mice and no *Dok-1*$^{-/-}$*Dok-2*$^{-/-}$ mice, exhibited abnormal accumulation of macrophages in the lung on necropsy at 8–12 weeks of age. Macrophages derived from *Dok-1*$^{-/-}$*Dok-2*$^{-/-}$*Dok-3*$^{-/-}$ mice displayed an exaggerated proliferative response to macrophage colony-stimulating factor (M-CSF) or granulocyte-macrophage colony-stimulating factor (GM-CSF) compared with WT and mutant controls. Together, these findings indicate that Dok-1, Dok-2, and Dok-3 cooperatively suppress aggressive HS, and commend *Dok-1*$^{-/-}$*Dok-2*$^{-/-}$*Dok-3*$^{-/-}$ mice as a useful model for the study of this neoplasia.

Laboratory Investigation (2010) **90,** 1357–1364; doi:10.1038/labinvest.2010.121; published online 14 June 2010

KEYWORDS: adaptor protein; Dok; macrophage; tumor

Histiocytic sarcoma (HS) is a malignant proliferation of cells showing morphological and immunophenotypic features of mature histiocytes, which represent tissue-resident macrophages.[1,2] Until recently, HS, which was also known as malignant histiocytosis, was often confused with anaplastic large B-cell lymphoma or with other malignant lymphomas. However, it has been established that true HS is a distinct and rare disease that is only about 0.1% as frequent as malignant lymphomas, which can be identified by the presence of B- or T-cell markers and/or CD30.[2] By definition, HS is negative for lymphocyte markers, but positive for histiocyte/macrophage markers such as CD163 in humans.[1,2] The tumor comprises a diffuse noncohesive proliferation of large cells, round to oval in shape, with abundant, eosinophilic cytoplasm and nuclear atypia. HS is an aggressive neoplasm with most patients dying of progressive disease. Patients may present with a solitary mass of HS, which is predictive of a relatively favorable outcome, but some patients show a systemic pattern of tumor spread.[1,2] As the molecular etiology of this disease is unknown, the development of rational therapeutics has been difficult. Although the generation of animal models is an essential step for the study of etiology, the paucity of mouse models that represent aggressive HS has remained an outstanding problem.

We and others previously identified Dok-1 as a common substrate of protein-tyrosine kinases (PTKs) including Bcr-Abl, a cause of chronic myelogenous leukemia,[3,4] and we further demonstrated that Dok-1 is a negative regulator of

[1]Division of Genetics, Department of Cancer Biology, The Institute of Medical Science, The University of Tokyo, Tokyo, Japan; [2]Department of Pathology, Tokyo Women's Medical University, Tokyo, Japan; [3]Novartis Institute for Biomedical Research, Cambridge, MA, USA; [4]Laboratory of Stem Cell Therapy, The Institute of Medical Science, The University of Tokyo, Tokyo, Japan; [5]Department of Developmental and Regenerative Biology, Medical Research Institute, Tokyo Medical and Dental University, Tokyo, Japan and [6]Department of Pediatrics, Center for Computational and Integrative Biology, Massachusetts General Hospital, Boston, MA, USA
Correspondence: Dr Y Yamanashi, PhD, Division of Genetics, The Institute of Medical Science, The University of Tokyo, 4-6-1 Shirokanedai, Minato-ku, Tokyo 108-8639, Japan.
E-mail: yyamanas@ims.u-tokyo.ac.jp

Received 20 March 2010; revised 19 May 2010; accepted 20 May 2010

PTK-mediated proliferation and transformation of cells.[5,6] Indeed, mice lacking both Dok-1 and its closest homolog Dok-2 developed a myeloproliferative disorder with a non-aggressive phenotype.[7,8] It is believed that Dok-1 and Dok-2 have virtually identical roles in myeloid lineages.[7–9]

The Dok family consists of seven members, Dok-1 to Dok-7, which share structural similarities characterized by the NH_2-terminal pleckstrin homology and phosphotyrosine-binding domains, followed by the src homology 2 target motifs in the COOH-terminal moiety, suggesting an adaptor function.[3,4,10–14] Among these members, only Dok-1, Dok-2, and Dok-3 are preferentially expressed in hematopoietic cells, or myeloid cells in particular, and comprise a closely related subgroup with regard to primary structure.[7,9,15] Similar to Dok-1 and Dok-2, Dok-3 is also a negative regulator of PTK-mediated signaling, despite being a relatively distant member of this subgroup.[11,16–19] However, mice lacking Dok-3 alone or Dok-1 and its closest homolog Dok-2 in combination do not develop aggressive tumors of hematopoietic cells.[7,8,18] In this study, we demonstrate that mice lacking Dok-1, Dok-2, and Dok-3 provide a model system for aggressive HS. Triple null mutant mice showed an early lethal phenotype that is associated with HS, and the tumor, which was transplantable, showed multiple organ invasion.

MATERIALS AND METHODS

Mice

Dok-1$^{-/-}$*Dok-2*$^{-/-}$ and *Dok-3*$^{-/-}$ mice were generated as previously described.[7,20] *Dok-1*$^{-/-}$*Dok-2*$^{-/-}$*Dok-3*$^{-/-}$ (TKO) mice were obtained by crossing *Dok-1*$^{-/-}$*Dok-2*$^{-/-}$ and *Dok-3*$^{-/-}$ mice (Supplementary Figure S1). Mice were genotyped by a standard PCR using DNA isolated from the tail tips. Primers to amplify the wild-type (WT) and targeted *dok-1*, *dok-2*, and *dok-3* loci have been previously described.[7,20] All mice were maintained in a mixed genetic background of strains 129/SvJ and C57BL/6 under pathogen-free conditions in the animal care facilities at Tokyo Medical and Dental University and The University of Tokyo. The experimental protocols have been approved by the animal ethics committees of the two institutions.

Histological Analysis

For hematoxylin and eosin (H&E) staining, tissue samples, aside from bones, were fixed in 10% neutral-buffered formalin, embedded in paraffin, sectioned, and stained. Bones were fixed similarly and decalcified in 14% EDTA solution for 3 days at room temperature with gentle stirring before staining with H&E. For immunohistochemistry using antibodies to Mac-2, PCNA, and Ki-67, paraffin sections were processed with 10 mM citrate buffer (pH 6.0) in a microwave (95°C, 15 min) and subjected to standard immunohistochemical staining using the streptavidin–biotin–peroxidase complex method. For immunohistochemistry using antibodies to F4/80, CD68, CD3, and B220, cryostat sections were fixed in 95% acetone at 4°C for 20 min and were also subjected to standard immunohistochemical staining using the streptavidin–biotin–peroxidase complex method. The slides were counterstained with hematoxylin. Endogenous peroxidase activity was inactivated by incubation with 3% hydrogen peroxide in methanol (at room temperature for 15 min). The following antibodies were used: anti-Mac-2 rat monoclonal antibody (M3/38, Cedarlane, Burlington, ON, Canada; dilution 1:400); anti-F4/80 rat monoclonal antibody (BM8, BD Biosciences, San Diego, CA, USA; dilution 1:100); anti-CD68 rat monoclonal antibody (FA-11, Serotec, Kidlington, UK; dilution 1:100); anti-B220 rat monoclonal antibody (RA3-6B2, BD Biosciences; dilution 1:100); anti-CD3 hamster monoclonal antibody (145–2C11, BD Biosciences; dilution 1:100); anti-PCNA mouse monoclonal antibody (PC10, Dako, Glostrup, Denmark; dilution 1:100); and anti-Ki-67 rat monoclonal antibody (TEC-3, Dako; dilution 1:50). Only nonautolyzed tissues from moribund or recently deceased mice were subjected to histological analysis.

Microscopy

Sections were viewed using an AX80 microscope (Olympus, Tokyo, Japan) with either a × 20 or × 40 PlanApo objective. Images were captured using a DP70 digital camera and DP Controller software (Olympus).

Transplantation

Nucleated bone marrow cells or splenocytes (2×10^6 cells) prepared from the donor were intravenously injected into lethally irradiated WT recipient mice. Irradiation was performed using an IBL-437C instrument (^{137}Cs, CIS Bio-International, Gif-sur-Yvette, France) at 9 Gy, and no survival was observed beyond 2 weeks after irradiation in the absence of transplantation. In Figure 3, TKO and WT mice at 78–88 weeks of age were used as donors and WT mice at 8–16 weeks of age were used as recipients. In Figure 4c, TKO and WT mice at 6–10 weeks of age were used as donors and WT mice at 8–16 weeks of age were used as recipients: these recipient mice were killed 8–10 weeks after transplantation and histological studies were performed.

Bone Marrow-Derived Macrophages

Bone marrow cells were cultured in DME medium containing 100 ng/ml of recombinant murine macrophage colony-stimulating factor (M-CSF, PeproTech, Rocky Hill, NJ, USA) and 15% FCS. After 7 days of culture, adherent cells were maintained in the absence of M-CSF for 16 h and were used as bone marrow-derived macrophages.

Cell Viability Assay

Bone marrow-derived macrophages (1×10^4) were plated in 96-well plates in quadruplicate, cultured in RPMI-1640 medium containing 15% FCS in the presence or absence of M-CSF or recombinant murine granulocyte-macrophage colony-stimulating factor (GM-CSF, PeproTech) for 5 days.

Cells were then treated with 3-(4,5-dimethyl-2-thiazolyl)-2,5-diphenyl-2H-tetrazolium bromide (MTT, Sigma, St Louis, MO, USA) for 4 h at 37°C, cellular formazan product was dissolved with acidic isopropanol, and the absorbance at 570 nm was measured spectrophotometrically to evaluate viable cells using an Emax microplate reader (Molecular Devices, Sunnyvale, CA, USA).

RESULTS

TKO Mice Succumb to HS

To examine whether Dok-1, Dok-2, and Dok-3 cooperatively suppress malignant tumor formation *in vivo*, we generated TKO mice. These mice were born at the expected Mendelian frequency without any abnormality in appearance evident by visual inspection. However, nearly half (15 of 33) of the TKO mice died between 14–51 weeks after birth, whereas all WT and *Dok-1*$^{-/-}$*Dok-2*$^{-/-}$ mice as well as all *Dok-3*$^{-/-}$ mice but one remained alive (Figure 1a). To gain insight into the early lethal phenotype of TKO mice, we first performed conventional histological studies. H&E staining of tissue sections revealed that TKO mice, but neither the other mutants nor the WT controls, showed a markedly high incidence (24 of 41) of large cell tumors at <65 weeks of age, characterized by the accumulation of abnormal cells with histiocytic morphology in the bone marrow, spleen, and/or liver (Figure 1b). The aberrant cells are distinguished morphologically from other hematopoietic cells by their round shape, prominent nuclear atypia, and eosinophilic cytoplasm, features that

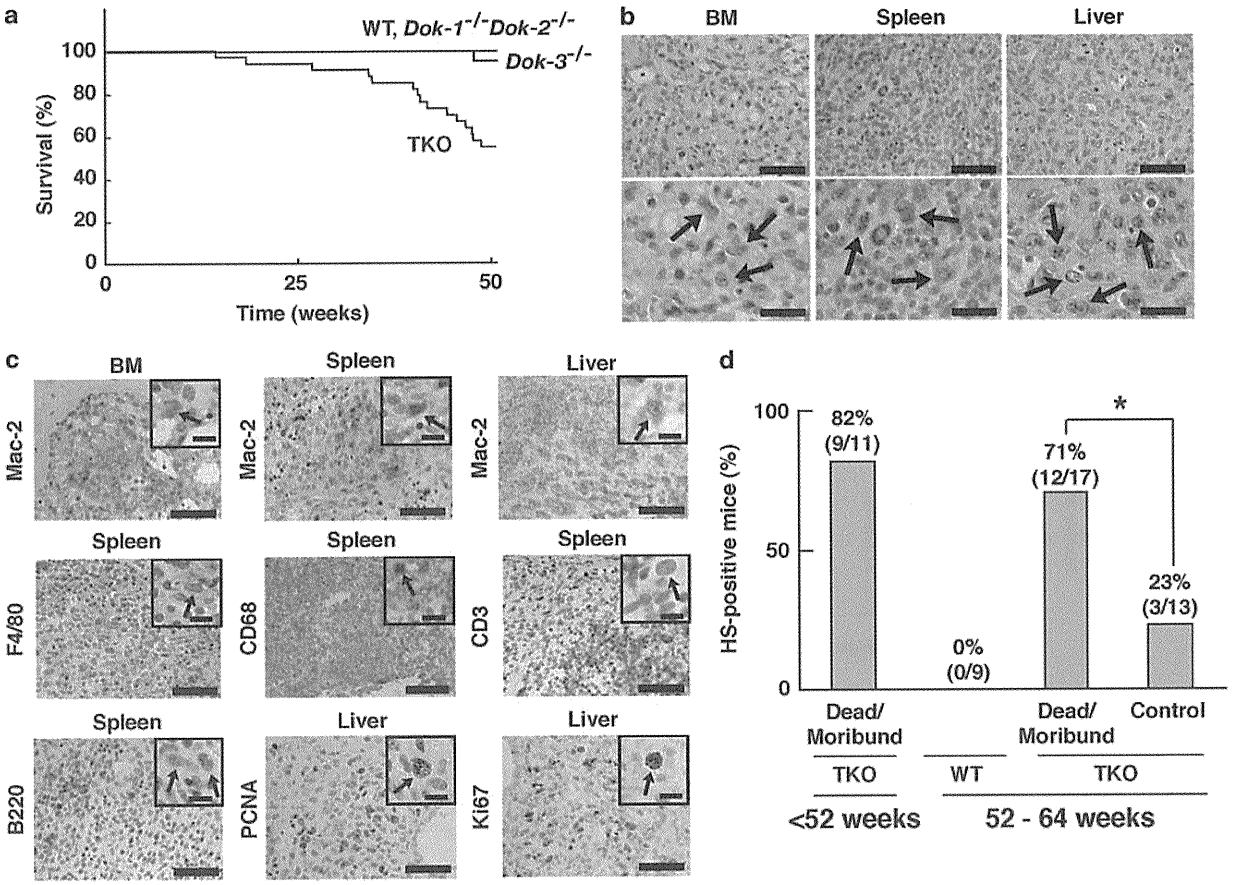

Figure 1 TKO mice develop HS with early mortality. (**a**) Survival of TKO ($n=33$), *Dok-1*$^{-/-}$*Dok-2*$^{-/-}$ ($n=20$), *Dok-3*$^{-/-}$ ($n=22$), and wild-type (WT, $n=26$) mice are presented. (**b** and **c**) Identification of tumor cells developed in TKO mice as HS by H&E (**b**) and immunohistochemical (**c**) staining. In panel (**b**), histology of tissue sections prepared from the bone marrow (BM), spleen, and liver of TKO mice is presented. Tumor cells are diffusely distributed (top), and are large and rounded and have atypical nuclei (bottom). Arrows indicate representative tumor cells. Scale bars show 100 (top) and 50 μm (bottom). In panel (**c**), tumor cells in the BM, spleen, and liver of TKO mice are stained with antibodies to Mac-2, F4/80, and CD68, but not by antibodies to CD3 and B220. Many of the tumor cells are stained with antibodies to PCNA and Ki67. Arrows indicate representative tumor cells. Scale bars show 100 and 20 μm (inset). (**d**) Association of the early lethal phenotype of TKO mice with HS. The percentage of mice that are HS positive in the BM, spleen, and/or liver was determined for each genotype and condition (dead/moribund or not) and is presented along with the exact fraction in parenthesis. Dead/moribund TKO mice at 52–64 weeks of age showed a significantly higher rate of HS positivity than TKO mice that were neither dead nor moribund (control). No tumor was observed in the age-matched WT mice. TKO mice that died or became moribund before 52 weeks of age also showed a high rate of HS positivity. Fischer's exact test was used to calculate the statistical significance. *$P<0.05$.

are characteristic of HS tumor cells (Figure 1b). Moreover, tumors showed monotonous morphology with tissue destruction and mass lesions, suggesting a malignant transformation (Figure 1b and Supplementary Figure S2). Immunohistochemical staining revealed the abnormal cells to be positive for the histiocyte/macrophage markers, Mac-2, F4/80, and CD68, but negative for the lymphocyte markers, CD3 and B220, consistent with the interpretation that these tumor cells represent HS (Figure 1c).[21,22] In addition, these cells stained positively with antibodies to MHC class II molecules, a marker of antigen-presenting cells including macrophages (Supplementary Figure S3). Further immunohistochemical examination showed HS cells to stain positively with antibodies to PCNA and Ki67, confirming that these cells are proliferative (Figure 1c).

As most patients with HS die of progressive disease, we examined whether HS is associated with the early lethal phenotype of TKO mice. As shown in Figure 1d, 9 of 11 moribund or dead mice at <52 weeks of age that could be necropsied bore HS in the bone marrow, spleen, and/or liver. Furthermore, no similar cells were found in WT mice even at 52–64 weeks of age. By contrast, 12 of 17 dead or moribund mice that could be necropsied at matched age developed HS, whereas only 3 of 13 nondead/moribund mice were positive for the tumor, indicating a significant link of HS with the lethal phenotype of TKO mice (Figure 1d).

HS Developed in TKO Mice is Highly Invasive and Transplantable

To evaluate the tumorigenic potential of HS developed in TKO mice, we wished to know whether the tumors spread into multiple organs. We examined six organs, the bone marrow, spleen, lung, skeletal muscle (femoral muscle), liver, and kidney. In all, 17 of the 21 tumor-bearing TKO mice at 25–66 weeks of age whose organs could be analyzed at necropsy showed multiple organ spread of the tumor (Figure 2a). As nearly all (20 of 21) TKO mice had HS in the bone marrow, this tissue might be the primary site of tumorigenesis in these mice (Figure 2b). Moreover, the majority (11 of 20) of bone marrow lesions were associated with osteolytic and direct invasions to the skeletal muscle (Figure 2b and c), indicating a strong invasiveness of the tumor. Next, to further examine the tumorigenic potential of HS developed in TKO mice, we examined whether the tumor was transplantable. Cells prepared from bone marrow or spleen of TKO mice or WT controls at 78–88 weeks of age were transplanted into lethally irradiated WT recipients intravenously. The mice transplanted with TKO cells from HS-positive tissues died within 10 weeks after transplantation, whereas control recipients that had been transplanted with cells from WT animals or from HS-negative sources of TKO animals survived, suggesting that the tumor was transplantable (Figure 3a). Indeed, histological study con-

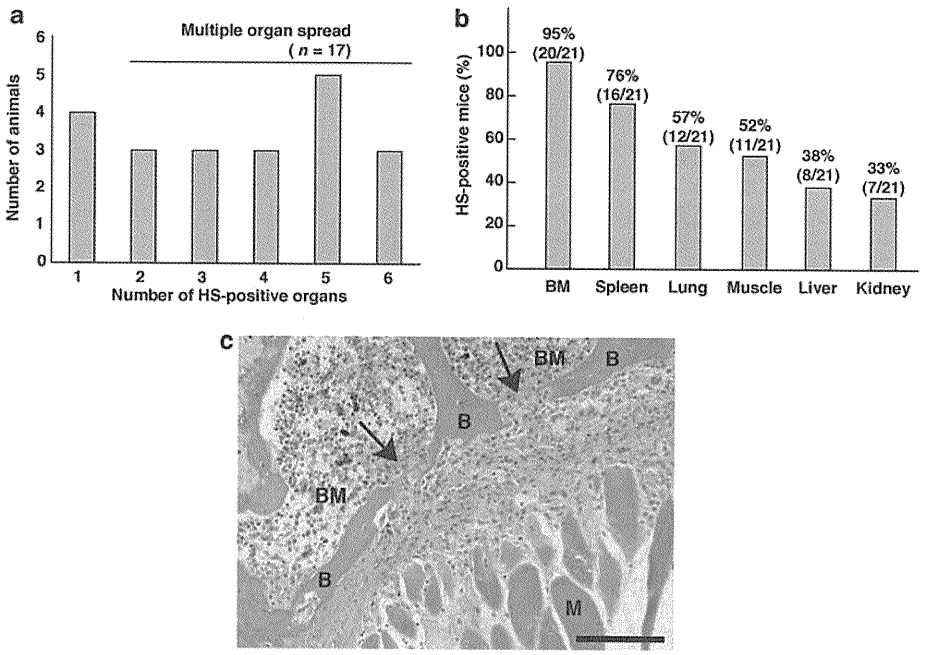

Figure 2 TKO mice show multiple organ spread of HS. (**a**) The number distribution of HS-affected organs in individual TKO mice. The bone marrow, spleen, lung, skeletal muscle, liver, and kidney from a total of 21 TKO mice were examined, and the number of HS-positive organs in each mouse was counted and plotted against the number of the corresponding mice. In all, 4 mice had only one HS-positive organ but the remaining 17 mice showed multiple organ spread of the tumor. (**b**) The organ distribution of HS positivity in TKO mice. From the data obtained in (**a**), the percentage of HS positivity by organ in affected mice is presented along with the exact fraction in parenthesis. (**c**) Histology of osteolytic invasions of HS into the skeletal muscle in TKO mice (H&E staining). B, bone; BM, bone marrow; M, muscle. Arrows indicate osteolytic lesions. Scale bar shows 100 μm.

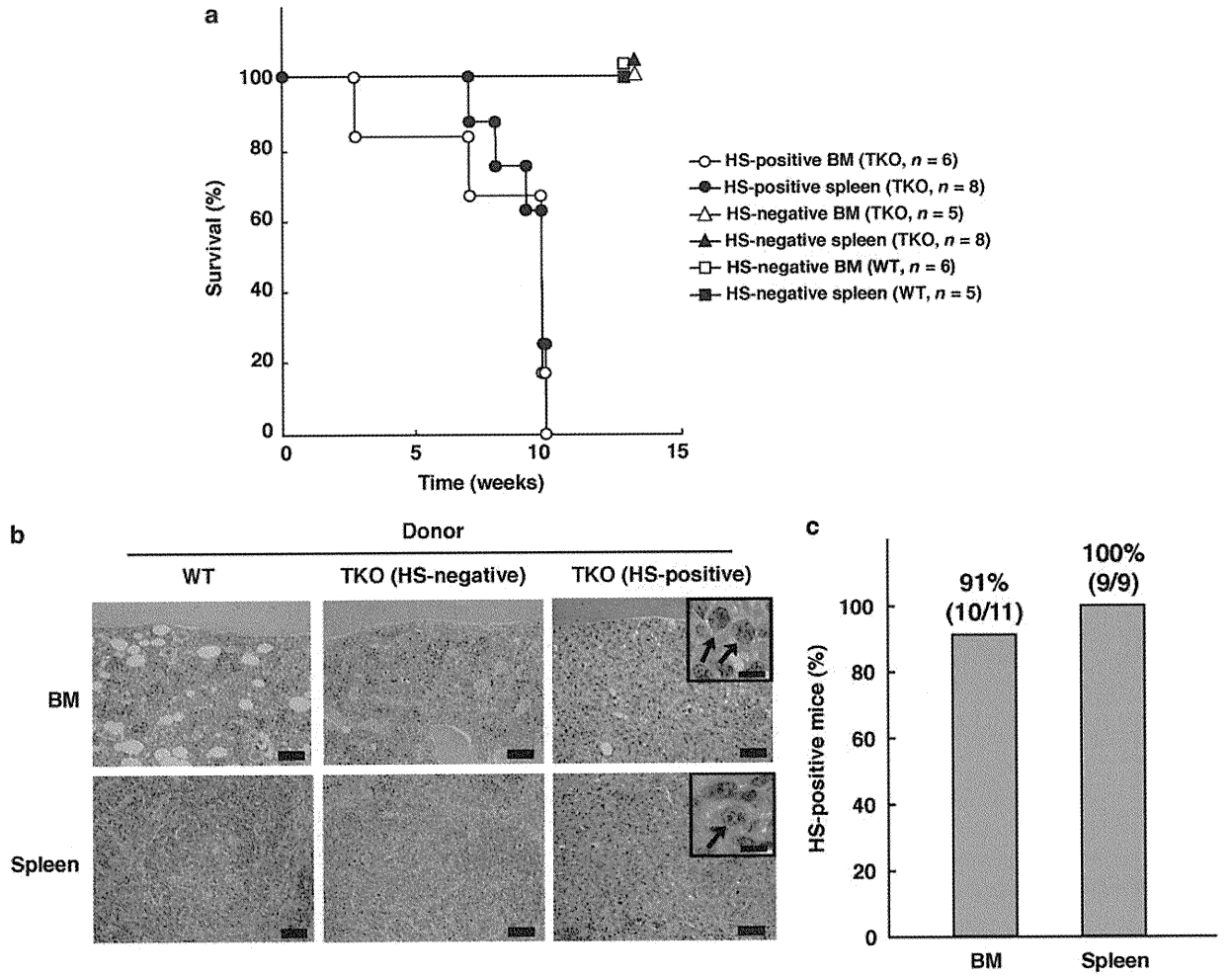

Figure 3 HS developed in TKO mice is transplantable. (**a**) Survival of transplanted mice. The survival rates of lethally irradiated (9 Gy) wild-type (WT) recipients that were transplanted with mononuclear cells from the bone marrow (BM) and spleen of the indicated donors are plotted against time after transplantation. The donor organs were scored as HS positive or negative, and only the recipients transplanted with WT cells or HS-negative TKO cells survived beyond 10 weeks after transplantation. (**b**) Histological analysis of transplanted mice. Histology of the BM and spleen sections prepared from the recipient mice that were transplanted with BM cells from the indicated donors is presented (H&E staining). Arrows indicate representative tumor cells. Scale bars show 100 and 20 μm (inset). (**c**) The percentage of HS-positive BMs and spleens in transplanted mice. The BMs and spleens from eleven and nine recipients, respectively, which had been transplanted with the HS-positive BM or spleen cells were examined. The percentage of HS positivity for BM and spleen was calculated and is presented along with the exact fraction in parenthesis.

firmed that almost all the recipient mice that had been transplanted with TKO cells from HS-positive animals and could be necropsied had HS in their bone marrow (10 of 11) and spleen (9 of 9) (Figure 3b and c). Furthermore, HS was not observed in control recipients that had been transplanted with WT cells ($n=11$) or TKO cells from HS-negative sources ($n=13$). We conclude that the malignant cell type that develops in TKO mice is highly invasive and transplantable.

TKO Mice Show Abnormal Accumulation of Macrophages in the Lung

During the course of histological analysis of TKO mice, we frequently found abnormal accumulation of Mac-2-positive macrophages in the lung (Figure 4a). These macrophages had a large cytoplasm without nuclear atypia and were not associated with tissue destruction, suggesting a non-tumorigenic nature. Almost all (13 of 14) TKO mice, but neither *Dok-1*$^{-/-}$*Dok-2*$^{-/-}$ (0 of 11) mice nor the WT controls (0 of 9), exhibited such abnormal proliferation of macrophages, which was uncorrelated with the presence or absence of HS at 50–59 weeks of age (Figure 4b). The incidence of macrophage accumulation in the lung was intermediate (3 of 8) in age-matched *Dok-3*$^{-/-}$ mice. Although development of lung adenocarcinoma, but not aggressive HS, has recently been reported in mice lacking Dok-1, Dok-2, and/or Dok-3 on a pure 129S1/SvImj genetic background even at the age of 11–15 months,[23] in this study mice mu-

tated in the same genes, but on a 129/SvJ and C57BL/6 mixed background, did not exhibit elevated incidence of lung adenocarcinoma. These different findings are likely due to the difference in the genetic backgrounds.

When bone marrow cells of TKO mice at 6–10 weeks of age were transplanted into lethally irradiated recipients, we invariably observed macrophage accumulation in the lung within 10 weeks after transplantation ($n=4$), but not when bone marrow cells were transplanted from WT controls (Figure 4c). Similarly, the histological study of TKO mice at 8–12 weeks of age, before the onset of observable HS, confirmed abnormal proliferation of macrophages in the lung of all mutant mice (8 of 8) but not in WT controls (0 of 8) (Figure 4d). Again no age-matched *Dok-1*$^{-/-}$*Dok-2*$^{-/-}$ (0 of 5) mice, and only a subset of *Dok-3*$^{-/-}$ mice (1 of 5), showed such accumulation of macrophages. Given that Dok-1 and Dok-2 negatively regulate proliferation of bone marrow-derived macrophages *in vitro*,[7] these findings suggest that Dok-1, Dok-2, and Dok-3 cooperatively inhibit the proliferation of macrophages.

Dok-1, Dok-2, and Dok-3 are Negative Regulators of Proliferative Response of Macrophages to M-CSF or GM-CSF

To address whether Dok-1, Dok-2, and Dok-3 are negative regulators of macrophage proliferation, we examined growth responses of bone marrow-derived macrophages from WT, *Dok-1*$^{-/-}$*Dok-2*$^{-/-}$, *Dok-3*$^{-/-}$, and TKO mice at 10–12 weeks of age on stimulation with M-CSF and GM-CSF, both of which are critical for proliferation of macrophages.[24–26] TKO

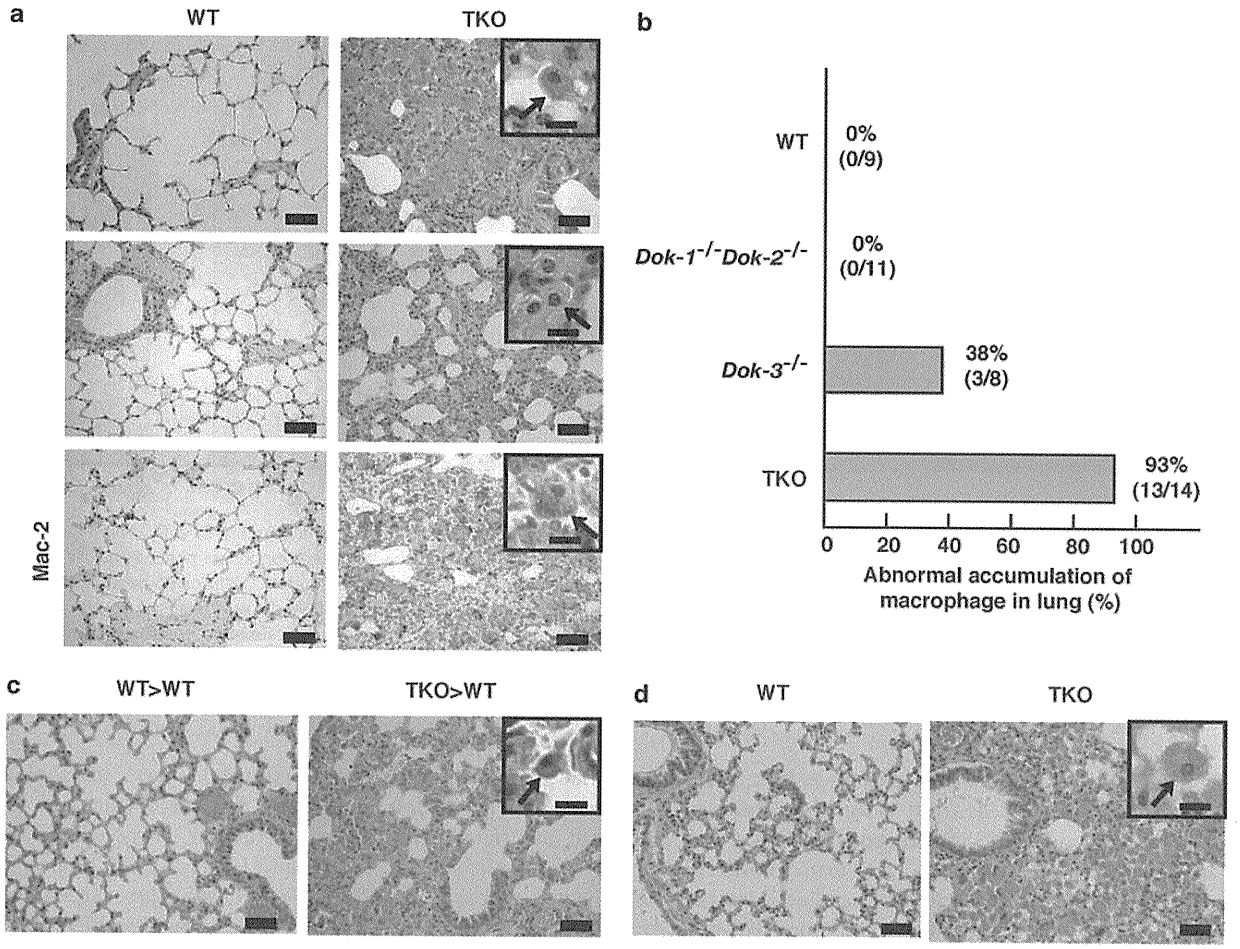

Figure 4 TKO mice show abnormal proliferation of macrophages in the lung. (**a**) Abnormal accumulation of macrophages in the lungs of TKO mice. Histology of lung sections prepared from wild-type (WT, left) and TKO (right) mice is presented (top, H&E staining; bottom, anti-Mac-2 staining). Arrows indicate representative macrophages present in the lung. Scale bars show 100 and 20 μm (inset). (**b**) The percentage of lungs with abnormal macrophage accumulations in various mice. The lungs from mice of the indicated genotypes were examined. The percentage of mice with abnormal lung macrophage accumulations was calculated and is presented along with the exact fraction in parenthesis. (**c**) Histology of lung sections prepared from recipient mice transplanted with bone marrow cells from WT (WT>WT, left) and TKO (TKO>WT, right) mice (H&E staining). An arrow indicates a representative macrophage present in the lung. Scale bars show 100 and 20 μm (inset). (**d**) Abnormal accumulation of macrophages in the lungs of younger (8–12 weeks of age) TKO mice. Histology of lung sections prepared from WT (left) and TKO (right) mice is presented (H&E staining). An arrow indicates a representative macrophage present in the lung. Scale bars show 100 and 20 μm (inset).

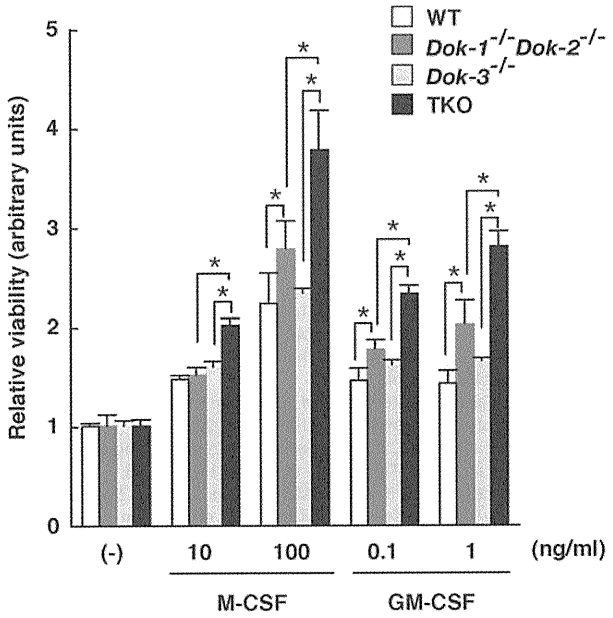

Figure 5 Augmented proliferative responses of bone marrow-derived macrophages prepared from TKO mice. Relative viabilities of bone marrow-derived macrophages of the indicated genotypes were evaluated by the MTT cell viability assay after 5 days of culture in the presence of M-CSF or GM-CSF at the indicated concentrations, in which the mean value in the absence of cytokine (−) was defined as 1 in arbitrary units for each genotype. WT, wild type. Data are expressed as mean ± s.d., and *P* values are calculated between WT and *Dok-1*$^{-/-}$*Dok-2*$^{-/-}$ or between TKO and *Dok-1*$^{-/-}$*Dok-2*$^{-/-}$ *or Dok-3*$^{-/-}$ macrophage proliferation. **P* < 0.05.

macrophages showed the highest proliferative response (Figure 5), consistent with the view that Dok-1, Dok-2, and Dok-3 are negative regulators of the proliferative response of macrophages to M-CSF or GM-CSF.

DISCUSSION

In this study, we have established that combined ablation of the adaptor proteins Dok-1, Dok-2, and Dok-3 has profound phenotypic consequences in mice. TKO mice, but not WT controls, develop and succumb to aggressive HS with multiple organ invasion. Although individual Dok proteins have the ability to inhibit PTK-mediated oncogenic signaling,[5–9,16] in this study mice lacking Dok-3 alone or Dok-1 and Dok-2 in combination did not develop aggressive tumors. The simplest interpretation for these data is that Dok proteins 1–3 can each suppress the aggressive transformation of HS. In addition, combined loss of Dok-1, Dok-2, and Dok-3 causes abnormal proliferation of macrophages in the lung, observable before the onset of morphologically recognizable HS. By contrast, combined ablation of Dok-1 and Dok-2 did not cause accumulation of macrophages in the lung. Although deficiency in Dok-3 caused abnormal proliferation of macrophages in the lung, the incidence was low. Therefore, the data suggest that these Dok proteins mutually compensate to inhibit the proliferation of macrophages. Indeed, our *in vitro* assay revealed that these proteins cooperatively downregulate proliferative response of macrophages on M-CSF or GM-CSF stimulation. Given that histiocytes are tissue-resident macrophages and HS is believed to arise from macrophage lineages, it is likely that the enhanced proliferative capacity of macrophages in mice lacking Dok-1, Dok-2, and Dok-3 contributes to the development of HS.

In general, Dok family proteins are believed to be activated as adaptors by tyrosine phosphorylation.[9] It was previously demonstrated that Lyn is required for the tyrosine phosphorylation of Dok-1 and Dok-3 in B cells (in which Dok-2 is typically undetectable) on B-cell receptor signaling,[6,27] suggesting that Lyn may activate these Dok proteins as negative regulators to suppress HS. Indeed, it has been reported that Lyn is expressed in macrophages, and that bone marrow-derived macrophages from Lyn-deficient mice showed enhanced growth responses to M-CSF and GM-CSF.[28] Furthermore, mice lacking Lyn develop macrophage tumors, which may be related to HS.[28] Unlike TKO mice, however, Lyn-deficient mice additionally develop severe renal disease.[29]

As mentioned above, HS in humans is an aggressive malignancy of unknown etiology and there remains a need for realistic animal models. Mouse models that have been reported for HS frequently show multiple lesions including lymphomas and severe renal failure. For example, the majority of mice lacking Pten, Ink4A, and Arf in combination develop both lymphoblastic B-cell lymphomas and HS with virtually the same incidence.[30] Similarly, mice lacking the cell-cycle regulator p21 develop a variety of tumors, including HS and B-cell lymphomas, and also suffered from severe renal failure,[31] unlike TKO mice. The syndrome elicited in mice lacking all the three proteins, Dok-1, Dok-2, and Dok-3, more specifically resembles the disease found in humans and hence may serve as a useful model for the study of HS. Although elucidation of the mechanisms by which the ablation of Dok proteins specifically causes HS and how the tumor gains its aggressive phenotype awaits further studies, such studies will help unveil the hidden etiology of this rare aggressive human malignancy.

Supplementary Information accompanies the paper on the Laboratory Investigation website (http://www.laboratoryinvestigation.org)

ACKNOWLEDGEMENTS

We thank Drs RF Whittier and T Yasuda for critically reading the paper and/or for thoughtful discussions; and Ms N Ogawa for animal care. This work was supported by Grant-in-Aid for Scientific Research on Priority Areas from the Ministry of Education, Culture, Sports, Science, and Technology of Japan.

DISCLOSURE/CONFLICT OF INTEREST

The authors declare no conflict of interest.

1. Grogan TM, Pileri SA, Chan JKC, *et al.* Histiocytic sarcoma. In: Swerdlow SH, Campo E, Harris NL, *et al.* (eds). WHO Classification of Tumours of